Using relative sea-level data to constrain the deglacial and Holocene history of southern Greenland

Sarah A. Woodroffe[1*], Antony J. Long[1], Benoit Lecavalier[2], Glenn Milne[2], Charlotte L. Bryant[3]

[1]Department of Geography, Durham University Science Laboratories, South Road, Durham, DH1 3LE, UK; s.a.woodroffe@durham.ac.uk; a.j.long@durham.ac.uk

[2]Department of Earth Sciences, University of Ottawa, Marrion Hall, Ottawa, K1N 6N5, Canada; b.lecavalier@gmail.com, gamilne@uottawa.ca

[3]NERC Radiocarbon Laboratory, Scottish Enterprise Technology Park, Rankine Avenue, East Kilbride, Glasgow, G75 0QF, UK, c.bryant@nercrcl.gla.ac.uk

*Corresponding author

Abstract

This paper presents new Holocene relative sea-level (RSL) data collected from isolation basins close to the town of Paamiut in south west Greenland. The data shows a rapid fall from a marine limit of c. 52 m asl at c. 10.9 cal. ka BP to close to present by c. 9.5 cal. ka BP, at rates of up to c. 32 mm/yr, falling below present for the majority of the Holocene before rising to present in the last 2000 years. The elevation of the RSL lowstand is not well constrained, but was at least below -3 m. This pattern of rapid RSL fall during the early Holocene matches the pattern seen at other southern Greenland locations suggesting rapid, largely simultaneous ice retreat from the area surrounding the Qassimiut Lobe at the start of the Holocene, occurring c. 2000 years after the initial deglaciation of the extreme southern tip of Greenland. The RSL histories from this and other southern Greenland locations are distinct to those recorded further north along the west coast, and are in broad agreement with a pattern of vertical land motion and RSL predicted by the Huy2 model (Simpson et al., 2009), which predicts an 80 m drop in the contribution of vertical land motion to RSL at 10 cal. ka BP between Sisimiut and Paamiut on the west coast. Despite this broad-scale spatial agreement between the RSL data and the Huy2 model, it fails to satisfactorily predict the Holocene RSL histories at Paamiut and other southern Greenland locations. Sensitivity tests indicate that the data-model misfits are most likely due to an over-estimate of the forcing during the Holocene Thermal Maximum (or the response to this forcing) in southern Greenland and error in the North American ice sheets component of the background deglaciation model. Our new data suggests that much of the southern part of the ice sheet acted differently to the area further north. However RSL changes at Paamiut are also largely impacted by regional and larger-scale processes including a bullseye of uplift centred on the west, the impact of the Holocene Thermal Maximum and the influence of the collapse of the North American ice sheets.

Keywords
Southern Greenland, relative sea level, deglaciation, isolation basin, geophysical model, Greenland Ice Sheet

1. Introduction

Our ability to model the past response of ice sheets to climate change is fundamentally dependent on the quality and distribution (in space and time) of geological observations of ice margin history and relative sea level (RSL) observations. In Antarctica, the relatively limited number of ice free locations around the perimeter of the ice sheet restricts the availability of RSL data, hindering efforts to determine rates of Holocene glacio-isostatic adjustment (GIA) that are needed to interpret present-day ice elevation changes and GPS observations (Whitehouse et al., 2012). By contrast, in Greenland an extensive ice free corridor around much of the ice sheet provides an excellent opportunity to develop a network of well constrained RSL observations that can provide powerful GIA constraints over the post-glacial period.

Since the late 1990s, several research teams have developed local Greenland RSL records based on the study of isolation basins, natural rock depressions that at various times in their history may be isolated from or connected to the sea by RSL change (see Long et al., (2011) for a recent review). These records show important regional variations in the timing, rate and direction of post-glacial RSL change that reflect, primarily, the interplay of local (Greenland ice sheet (GIS)) and non-local ice loading (Tarasov and Peltier, 2002; Fleming and Lambeck, 2005; Simpson et al., 2009).

Despite these recent RSL studies, we still lack good quality observations from large sections of the ice-free Greenland coast. In west and south Greenland, published studies suggest two types of RSL history. In the far south of Greenland, in the region of the Qassimiut Lobe and the Julianehåb Ice Cap (Figure 1), RSL typically fell very rapidly from the local marine limit following deglaciation and reached present sea-level by the early Holocene. RSL continued to fall below present (by up to ~10 m in places) before rising to present by an equivalent amount from the mid Holocene onwards (e.g. Sparrenbom et al., 2006a, b). This latter rise has been interpreted to record the combined effects of the collapse of the Laurentide forebulge, which extends beneath much of Greenland, and also the expansion of the Greenland Ice Sheet (GIS) in the neoglacial that caused renewed crustal loading and glacio-isostatic depression (Kelly, 1980; Long et al., 2009). This type of RSL curve was described by Clark et al (1978) as their 'Transition zone between I and II' occurring at and close to the margins of former ice sheets. They suggest it arises where initial rapid RSL fall occurs on glacial retreat due to the combination of elastic rebound and the relaxation of the gravitational attraction of the ocean by diminishing ice mass through time. This is followed by RSL rise caused by the slowing of rebound and the gravitational effect, and submergence due to the collapse of the local glacial forebulge. They predict a larger initial RSL fall and smaller later RSL rise for sites that are closer to the former ice sheet.

A different type of RSL record is observed further north and along much of the west coast of Greenland at least as far north as Disko Bugt (Figure 1). Here the pattern typically resembles a J-shape, resembling Clark et al's 'Type I' curve, with RSL also falling rapidly in the early- and mid-Holocene but staying above and only reaching present sea-level during the mid or late Holocene. Often there is a small RSL lowstand (up to c. -5 m at sites close to the present ice sheet margin) followed by a late Holocene RSL rise to present (e.g. Long et al., 2006). This type of RSL record is predicted for formerly glaciated areas where there is fast initial RSL fall due to both ice load removal and the reducing gravitational attraction of the ocean, but these processes are largely offset the effects of the passing forebulge in the mid-late Holocene. These processes result in RSL to rise by less than in sites located further from the ice margin.

Although both the west (Type I) and south (Transitional Type I-II) regions of Greenland were ice-covered at the Last Glacial Maximum (LGM) (Simpson et al., 2009), the difference in ice load and the chronology of unloading between these two locations has created curves that resemble Clark et al's (1978) modelled Type I (previously glaciated) and Transitional Type I-II (ice margin) RSL histories. In west Greenland the ice load was larger compared to that in south Greenland, causing a higher marine limit and more RSL fall in the early Holocene. In contrast, although south Greenland experienced a smaller ice load and less rebound, here the effects of forebulge collapse associated with both Greenland and the former Laurentide Ice Sheet combine to control RSL change.

The ongoing debate is where along this coast the transition between these two different RSL curves occurs. This has implications for reconstructing the volume of ice present over west Greenland at the LGM and its evolution and decay through time. A spatial plot of RSL variability in Greenland at 10 cal. ka BP produced by the Huy2 model of the evolution of the GIS (Simpson et al., 2009) shows a drop in the contribution of vertical land motion to RSL by 80 m at 10 cal. ka BP between Sisimiut and Paamiut (Figure 2). This predicted change will have affected RSL and is likely to have caused a transition between a Type I and Transitional Type I-II RSL curve over a broad zone of south west Greenland between Sisimiut and Paamiut (Figure 2). However a previous study by Weidick et al. (2004) uses RSL data from south west Greenland to suggest that a gradual transition between Type I and Transitional Type I-II RSL histories occurs further south between Paamiut (Type I) and Qaqortoq (Transitional Type I-II), although the precision of the Paamiut RSL observations is not good (discussed below). It has not been possible until now to test these two different models of RSL change because of the limited spatial distribution of RSL observations and their varying precision along this stretch of the southern Greenland coast. The new data presented in this paper allows us to constrain the spatial distribution of these two models of RSL changes in west and south Greenland.

A second aim of this paper is related to the Huy2 model of evolution of the GIS which is used to model RSL along this coast. Although the Huy2 model is tuned to Holocene RSL data from west Greenland (Simpson et al., 2009), it does not closely predict Holocene RSL changes at sites in south Greenland (e.g. at Qaqortoq and Nanortalik (Figure 3)). In this paper we determine through comparison with new RSL data from Paamiut and a sensitivity study, how model revisions can improve the accuracy of the Huy2 model in south Greenland.

In this paper we develop a RSL record from Paamiut using newly collected isolation basin RSL data that, in conjunction with existing RSL data and modelling experiments using Huy2 (Simpson et al., 2009), allows us to discriminate between the two models of Holocene RSL change in south Greenland outlined above. The work is important because changes to the Huy2 model in south Greenland suggested by this study will help improve our ability to understand the driving mechanisms responsible for responses of the GIS to climate and other forcings over millennial timescales, and help better isolate the background GIA trend as required in the interpretation of geodetic observations (e.g. GPS, satellite gravity) for contemporary ice sheet change.

2. Study area and previous work

The southern part of the GIS is made up of the main ice sheet (the inland ice) and several contiguous ice caps and ice lobes, notably the Qassimiut Lobe and the Julianehåb Ice Cap (Figure 1). The bedrock terrain beneath the southern part of the ice sheet is generally high (between 1000 and 2000 m) compared with areas to the north where bedrock relief beneath the main ice sheet is much lower, typically <500 m and in places below sea-level. Another difference is that in the far south of Greenland the continental shelf is relatively narrow (40-60 km) compared to areas further north where it reaches c. 120 km (e.g. offshore from Sisimiut (Figure 1)).

Paamiut lies c. 250 km south of Nuuk and 320 km north west of Nanortalik (Figure 1). The northern edge of the Qassimiut lobe is about 100 km to the south east. There is a 40 km-wide ice free coastal corridor between the outer coast and the ice sheet margin and the intervening terrain comprises uplands that reach elevations of c. 800 m that are dissected by steep-sided fjords. An existing RSL curve for Paamiut comprises six radiocarbon dates from gytjja that overlies marine sediment in isolation basins (Anderson et al., 1999; Kelly and Funder, 1974; Tauber, 1968; Weidick et al., 2004). The dates have no supporting biostratigraphic information and the original elevations for five of the lakes reported in Tauber (1968) are revised upwards by up to 14.5 m by Weidick et al. (2004) because of problems with the original survey data (Michael Kelly, pers. comm. 2009). The lakes from which the samples were obtained are located c. 10 km to the north of Paamiut (Figure 1b). Two additional lakes lie above the marine limit and suggest the first establishment of ice free conditions in the area by c. 11 cal. ka yr BP (Anderson et al., 1999; Kelly and Funder, 1974) (Figure 1).

The new RSL data described in this paper come from a low-lying island, 12 km south east of Paamiut. The bedrock geology comprises Pre-Cambrian gneiss and the tidal range at Paamiut is 3.6 m (pers. comm. Danish Marine Safety Administration, 2009). Mean High Water of Spring Tides (MHWST) and Highest Astronomical Tide (HAT) are ~1.4 m and ~1.8 m above Mean Tide Level (MTL) respectively. The area has an annual mean temperature between 1961-1990 of -0.8°C (summer mean 4.9°C, winter mean -6.1°C (Box 2002)).

3. Methods

We cored one lake above the local marine limit, four isolation basins at a range of elevations between 39 m and 1.99 m above MTL, and two submerged isolation basins with sills currently in the intertidal zone. We recorded the stratigraphy of the lake sediment sequences using transects of cores completed with a hand operated gouge and Russian-type corer operated from a tethered boat. We retrieved samples cores from the lakes using a hand-operated piston corer. All altitudes were surveyed using a level and staff with closed levelling transects that were tied to a common reference point that we related to MTL using tidal predictions for Paamiut that were confirmed using a sea-bed pressure transducer for the 3 week period of fieldwork. For each basin we surveyed the minimum and maximum sill elevations, and quote the mid sill elevation plus and minus an error term which relates to the range of the indicative meaning of each dated sample and the measurement error in the paper. The sill height is the critical elevation which controls basin isolation and ingression.

We analysed diatoms from the sample cores to determine different stages in basin isolation and ingression (see Long et al., (2011) for a review of isolation basin methods). Typically the sample cores contained insufficient macrofossils to date the point of basin isolation so we instead used AMS radiocarbon dating of 0.5 cm thick bulk sediment slices from immediately above the isolation contact. The dated isolation contact was not always at the first occurrence of clay gyttja in the lake core, but always at the diatomological isolation contact where we can define the indicative meaning of the sediment as between MHWST and HAT. The geology of the area is Archean basement with no sources of old carbon in the catchments or within the lake basins themselves. Comparison of cosmogenic isotope ages from bedrock and boulders and basal lake ages elsewhere in west Greenland (Larsen et al., In press) suggests that the onset of organic accumulation in lake basins above the marine limit can postdate deglaciation by up to ~1300 years and therefore the age of lake P62 provides a minimum age for local ice retreat only. The isolation basin dates from below the marine limit provide a precise age estimate of RSL.

Radiocarbon dating was undertaken at the SUERC AMS Laboratory at East Kilbride, Scotland, and ^{14}C dates are all calibrated using the Oxcal program version 4.1 (Bronk Ramsey, 2009) using INTCAL 09 (Reimer et al., 2009) and cited with a two sigma age range (Table 1).

4. Results

We surveyed the height of the local marine limit by measuring the elevation of the transition between wave-washed rock and perched boulders at 16 locations close to our sampled lakes. This yielded an elevation in the range of 51.7-53.4 m above MTL. This limit was formed by a MTL of c. 50-52 m asl, assuming no change in tidal range from the present.

Freshwater gyttja began forming in basin P62, a short height above the local marine limit at or before 10,480-10,231 cal. yr BP (Figure A1 and Table 1). This is younger than deglacial ages from other lakes above the marine limit in the area (c. 10,900 cal. yr BP, Anderson et al., 1999; Kelly and Funder, 1974) and is also younger than our oldest isolation contact (see below). The P62 date is therefore a minimum age for local ice free conditions.

Isolation contacts in basins P38 (38.82 m MTL), P24 (24.86 m MTL), P12 (12.23 m MTL) and P2 (1.99 m MTL) all record basin isolation and RSL fall between c. 11 and 9.5 cal. ka yr BP. Summary diagrams showing the change in diatoms from fully marine (polyhalobian), through brackish (mesohalobian) to freshwater species (oligohalobian-indifferent and halophobous) across the isolation contacts in each basin are in Figure 4. Dates are listed in Table 1 (full details of diatom analyses are found in the supporting information, Figures A2-A11). The sedimentary contact in lake P38 is sharp and there is a thin sand layer at the isolation contact. We dated material immediately below the sand layer and therefore the isolation age of this lake (11206-10800 cal. yr BP) is a maximum age for isolation of this basin. We are confident that the diatom assemblages from the other basins show gradual isolation with no evidence of erosion and therefore the reported ages in all but lake P38 relate to the timing of final isolation and not to pre-isolation conditions or a later colonisation of the lake (Figure 4). The stratigraphy of the two tidal ponds is more complex because they have experienced complex depositional histories and each is now described in detail.

The sill of Basin P0 (0.64 m above MTL) is within the upper part of the present intertidal zone, evidenced by salt marshes around the lake periphery. The lower part of the lake stratigraphy is a grey silt/clay which is overlain by green silt gyttja (Figure Figure 4 and A12). Diatoms across this contact show an up-core change from marine to freshwater conditions and basin isolation is dated at 558.5-559 cm to 9470-9258 cal. yr BP (Figure 4 and Table 1). The freshwater gyttja above this is c. 1 m thick and changes in the top 0.4 m to a slightly more minerogenic deposit. Diatoms in the main freshwater deposit are dominated by oligohalobian-indifferent *Fragilaria spp.* and *Eunotia spp.* A sample of gyttja at 475-475.5 cm yields an age of 2349-2156 cal. yr BP. At 462 cm there is a transition to a slightly brackish diatom assemblage, with the first occurrence of low numbers of polyhalobian and mesohalobian taxa (Figure 4 and A9). This records the renewal of tidal inundation into the basin, most probably initially by storms waves. A sample of gyttja from 462-462.5 cm dates the first occurrence of marine and brackish taxa to 1393-1292 cal. yr BP (Figure 4).

Basin P-1 (-0.9 to -1.25 m below MTL) has a sill between MLWNT and MLWST and fills and partly drains on each tide. A transect of cores across the lake records a lower silt/clay overlain by c. 2.3 m of green gyttja that passes upwards into a slightly more minerogenic gyttja in the uppermost 0.6 m (Figure 4 and A13). Diatoms across the isolation contact show a rapid change from marine to freshwater conditions, dated at 888.5-889 cm to 9548-9482 cal. yr BP. An ingression contact is recorded towards the core top by an increase in poly- and mesohalobian diatoms. Although there are only low numbers of marine diatoms in the core until 653 cm, we interpret the first occurrence of marine species at 657 cm as indicating that the basin has entered the intertidal zone. A sample of silty gyttja from 657-657.5 cm dates this first marine flooding to 931-775 cal. yr BP.

5. Local and regional trends in relative sea-level in south and west Greenland

Our new RSL data from Paamuit show RSL fell rapidly from a local marine limit of c. 52 m at or before c. 10.9 cal. ka BP to close to present by c. 9.5 cal. ka BP, at a rate of c. 32 mm/yr (Figure 5A). The lake above the marine limit (P62) only provides a minimum age for local ice retreat as there is often a lag between deglaciation and organic accumulation in lake basins above the marine limit (Larsen et al., In press). RSL continued to fall and remained below present for the rest of the Holocene. We need further deep-silled basins to establish when and at what depth the Holocene RSL lowstand was reached, but based on the rapid early Holocene fall and rate of late Holocene RSL rise of c. 3 mm/yr since 1 cal. ka yr BP, we suspect it must lie at least -5 to -10 m below present and likely dates from the mid Holocene (see below).

Our new RSL data are very different to those from previous studies in the Paamiut area (Figure 5B, Anderson et al., 1999; Kelly and Funder, 1974; Tauber, 1968; Weidick et al., 2004). We think this reflects problems with the original data rather than any real differences in RSL between the two local study areas at Paamiut. Tauber (1968) used conventional radiometric dates from bulk sediment slices up to 5 cm thick, and in one case aggregated material from three adjacent boreholes. This may have introduced material younger than the date of basin isolation into the age determinations. We date an individual thin (0.5 cm thick) sediment slice from each lake to minimise these potential errors. Weidick et al. (2004) revised the altitude of five index points upwards by up to 14.5 m from their original publications but this increases rather than decreases the vertical discrepancy between these and our new data. The sea-level index point reported by Anderson et al. (1999) from a basin north of Paamiut at c. 17 m asl fits closely with our new RSL data (Figure 5B), further suggesting that there are problems with the older data not that they record significantly different RSL as they sit closer to the former centre of uplift in west Greenland (Figure 2).

Our Paamiut record is similar to other Transitional Type I-II RSL records from the southern tip of Greenland. There is no change, as hypothesised by Weidick et al. (2004), between Transitional Type I-II and Type I RSL histories within the wider study area that extends between Paamuit and Nanortalik. Thus, the rapid fall during the early Holocene, from a local marine limit at ~50 m asl is closer in timing and rate of fall to RSL records from Qaqortoq and Nanortalik than from locations further north, such as Sisimiut where RSL fell from a much higher marine limit around 1000 years later (Figure 3) (Sparrenbom et al., 2006 a,b). RSL reached present at Paamiut at c. 9.5 cal. ka BP, and between 9.5-8.9 cal. ka BP at other southern sites. RSL was below present at Paamiut, as elsewhere in southern Greenland, for the majority of the Holocene.

6. Comparisons of RSL data and Greenland ice sheet models

6.1 Regional ice sheet models

Studies by Bennike et al. (2002) and Sparrenbom (2006) use isolation basin data from Nanortalik and/or Qaqortoq to constrain ice sheet models for southern Greenland since the LGM. These models use locally prescribed deglacial chronologies and a range of different earth models that are varied to obtain an optimum data/model fit. The models consist of an idealised axi-symmetric ice sheet with parabolic or quasi-parabolic radial height profiles and prescribed ice margin configurations through time. Sparrenbom's (2006) model also includes load from Greenland and non-Greenland sources and assumes a pre-LGM load history and inheritance. Both models set the LGM extent at the shelf edge, with fast and late ice retreat across the shelf between 15-14 cal. ka BP (Bennike et al., 2002) or 15-12 cal. ka BP (Sparrenbom, 2006), reaching the present coast at Paamiut between 14-12 cal. ka BP with no Younger Dryas readvance.

In the Paamiut area, Sparrenbom's model predicts rapid RSL fall during the early Holocene, more closely matching the RSL data than the Huy2 model described below (Figure 5B). The model also predicts that RSL was falling prior to the area becoming ice free whereas Huy2 predicts RSL rise during the period 14-11 cal. ka BP (Figure 5B). Sparrenbom's model then predicts RSL falling below present and remaining there for much of the Holocene. This relies on the ice margin obtaining its minimum position of 40 km inland of its present position by 9 cal. ka BP, and readvancing to its present position by 5.5 cal. ka BP. The timing of this readvance is early relative to the evidence from the DYE3 ice core that the HTM was between 6-3 cal. ka BP in southern Greenland (Dahl-Jensen et al., 1998), and also a range of palaeoclimate data from terrestrial records that suggest cooling began after c. 4.5 cal. ka BP (Kaplan et al., 2002; Larsen et al., 2011; Massa et al., 2012). Although this regional model provides a coherent fit between data and observations in southern Greenland, it relies on tightly prescribed ice margin and thickness data and lacks a physically realistic, 3-D thermo-mechanical model of ice sheet evolution. It is specific to southern Greenland and cannot easily be extended to capture the evolution of other parts of the GIS.

6.2 Greenland-wide ice sheet models

Three Greenland-wide ice sheet models have been developed that use RSL data to constrain the magnitude and timing of ice retreat from the LGM maximum, the minimum size of the ice sheet during the Holocene Thermal Maximum (HTM) and the mid-late Holocene neoglacial advance (Fleming and Lambeck, 2004; Simpson et al., 2009; Tarasov and Peltier, 2002). Two of these studies (Tarasov and Peltier 2002, Simpson et al., 2009) use a 3-D thermomechanical ice sheet model driven by prescribed climatic data (from the GRIP ice core) which freely simulates past ice sheet evolution.

We focus on the most recent model (Huy2, Simpson et al., 2009), which achieves a reasonable fit to the RSL history at Sisimiut on the west coast but provides a poor fit at Paamiut, Qaqortoq and Nanortalik in the south (Figure 3 and 5B). The misfit between model and data in this region is the greatest seen across all of Greenland (see Figure 16 in Simpson et al., 2009). At Paamiut the model does not replicate the very fast, early Holocene RSL fall between c. 11-9.5 cal. ka BP, nor the prolonged period of RSL below present through the Holocene. The modelled RSL at 6 cal. ka BP for Paamiut is at c. 20 m. Assuming that the mid Holocene RSL lowstand at Paamiut was between -5 and -10 m, this means that Huy2 overpredicts RSL at this time by 25 m to 30 m. We hypothesise that the reasons for this mis-match lie either in the local (Greenland) Earth and ice models and/or in non-Greenland parameters, notably the effects of the Laurentide forebulge. In the following we explore the poor fit of Huy2 at Paamiut by considering both field evidence and model sensitivity tests.

6.2.1 Earth model parameters

Relative sea-level predictions in Greenland, as elsewhere, are sensitive to Earth model parameters, especially upper mantle viscosity (Simpson et al., 2011). To test for this we compute RSL predictions at Paamiut using a broad range of Earth viscosity values (Figure 6A), considering only viscosity models that produced an equivalent (to 95% confidence) and high-quality fit to the entire regional Greenland data set considered in Simpson et al. (2009). This included a sub-set of 8 models out of several hundred considered; of these 8 models, predictions for 3 are shown in Figure 6A. It is evident that none of the solutions is able to replicate the millennial scale pattern of our Holocene RSL data. The model with relatively low viscosities (grey line) enhances the local land uplift and so better fits RSL in the early Holocene. However, this results in an ever poorer fit during the mid and late Holocene when sea levels were below present. The predictions in Fig. 5A suggest that a more probable cause of the mis-fit is error in the ice load model.

6.2.2 Changes in timing of local ice retreat

The local ice history in Huy2 south of 63°N on the west coast predicts ice extending to the shelf edge at the Last Glacial Maximum (LGM), retreating from 16 cal. ka BP to reach the present coastline by 14 cal. ka BP, with a Younger Dryas re-advance close to the shelf edge again at 12 cal. ka BP. By 10 cal. ka BP ice has retreated onshore, reaching its current margin by 9 cal. ka BP. The model predicts a small retreat (20 km) inland during the HTM with a minimum extent by 4 cal. ka BP followed by a late Holocene re-advance to its present margin. This ice history is significantly different to that used in Sparrenbom's regional ice model, which has much earlier ice retreat (to the present coast by 14-12 cal. ka BP), with no Younger Dryas eadvance and the ice margin 40 km inland of its present position by 9 cal. ka BP.

There is limited field evidence to provide independent testing of the early deglacial ice margin positions and for this reason validating the Huy2 ice sheet model is difficult. The presence of low relief banks on the outer shelf, comprising sands and gravels and coarse clasts of likely glacial or glaciomarine origin, probably record the Last Glacial Maximum (LGM) ice position (Weidick et al. 2004). Offshore of Paamiut these are mapped as the Narsalik Banke but they are not dated and may have a complex origin (Weidick et al., 2004). A high level weathering zone is identified onland in the Paamiut area, although its geomorphological significance is debated. Kelly (1985) and Weidick et al. (2004) interpret this limit as a trim line formed during the Neria Stade which they correlate with ice sheet readvance onto the shelf during the Younger Dryas. However, others suggest that it more likely records a thermal boundary between warm and cold ice (Bennike and Björck, 2002; Björck et al., 2002; Carlson et al., 2008; Funder et al., 2011; Larsen et al., 2011). Our data provide no new insights into whether there was a Younger Dryas readvance of the GIS in the Paamiut area, but does confirm this area became ice free at or before c. 11 cal. ka BP which would have required rapid ice retreat from the 12 cal. ka BP shelf-edge position. The RSL data also suggests that the ice sheet retreated rapidly inland from the Paamiut area to produce very rapid RSL fall in the early Holocene. The ice history in Sparrenbom's 2006 model suggests earlier ice retreat compared to Huy2 but also significant in situ melting over the late glacial period creating at least 20 m of RSL fall prior to deglaciation (Figure 5B).

Evidence from marine cores, offshore southern Greenland, for the position of the ice sheet during the Younger Dryas is also unclear. Knutz et al., (2011) investigated ice rafted debris (IRD) in a marine core south west of Nuuk in the Labrador Sea and suggest from low ice rafted debris (IRD) levels during the Younger Dryas period that dense sea ice may have restricted the offshore movement of icebergs. They also speculate that the ice margin may have been on the shelf at this time. Carlson et al. (2008) also analyse a marine core from further south in the Labrador Sea, and show raised Fe and Ti levels throughout the Younger Dryas, suggesting that this cold period did not affect the ongoing ablation of the southern part of the ice sheet.

Regardless of the lack of field data to test the accuracy of the model prediction, it is possible to carry out sensitivity tests to determine if altering the late glacial and early Holocene margin chronology can account (in part or completely) for the large data-model misfits described above. By varying the severity of the sea-level forcing in the ice model, two additional retreat scenarios are produced that include earlier retreat (margin land based by ~14 cal. ka BP or ~11 cal. ka BP) than in the original Huy2 model (margin land based by ~10 cal. ka BP). Results show higher marine limits are predicted the later the margin retreats from the shelf (Fig. 5B). These results indicate that while this aspect of the model cannot resolve the large data-model residuals, the data do support a late retreat of the ice margin in this area. The scenario with early retreat (dashed line in Figure 6B) also does not include a significant Younger Dryas readvance of the ice sheet onto the shelf. In the other two scenarios the ice sheet readvances onto to the mid shelf in the ~11 cal. ka BP scenario (grey line in Figure 6B) and to the LGM position in the Huy2, ~10 cal. ka BP retreat scenario (black line in Figure 6B). Our RSL data suggests that the Huy2 solution with late retreat to the land (by 10 cal. ka BP) is incorrect, but predictions using earlier retreat lower the height of the marine limit, decreasing the model fit to the RSL data. Importantly none of the Huy2 predictions predict RSL fall prior to deglaciation, which is an important aspect of Sparrenbom's 2006 model that contributes to its good fit to our RSL data during the early Holocene (Figure 5B). This process could be considered in future analyses of ice sheet evolution in this region.

6.2.3 Intensity of Holocene thermal maximum retreat

The modelled late Holocene readvance of the ice sheet has an important impact on modelled RSL predictions in the Disko Bugt area. Fleming and Lambeck (2004) showed previously how the inclusion of a neoglacial ice sheet readvance causes RSL predictions in Disko Bugt to fall below present in the late Holocene and fit RSL observations (Long et al., 1999), but neither their tuned model, nor that of Tarasov and Peltier (2002) include a neoglacial readvance of the Qassimiut Lobe. A more recent modelling study using ICE-5G suggests that a 33 km readvance of the Qassimiut Lobe during the last 3 k yr is needed to explain present-day GPS measurements of land uplift (Khan et al., 2008). In contrast, although the Huy2 model of Simpson et al. (2009) includes a 20 km neoglacial readvance in the south, this is too small

(Simpson et al., 2011) to generate the timing and magnitude of the RSL lowstand which, at Nanortalik and Qaqortoq, is the largest seen in all of Greenland (up to -10 m at c. 6 cal. ka BP; Sparrenbom et al., 2006b).

Sedimentological data collected from threshold lakes (which record periods of inwash of glacial sediment caused by ice sheet advance / retreat) provide no clear evidence for a large readvance of the entire Qassimiut Lobe. At Lower Norbosø, close to Narssarssuaq, Larsen et al. (2011) suggest only modest ice margin changes during the mid and late Holocene and a dampened climate response compared with that proposed by Weidick et al. (2004). In the west of the region, at Qipisarqo, Kaplan et al. (2002) record the inwash of glacial sediment into a lake close to the margin of the present ice sheet only at the start of the Little Ice Age suggesting a late readvance in this area. Given these observations, and that the RSL lowstand is a feature common to all RSL study sites in the vicinity of the Qassimiut Lobe, additional neoglacial loading to that included in the Huy-2 model would seem improbable. The conclusion is that additional neoglacial loading was not an important contributor to the low values of RSL observed during the Holocene.

Viewed at a larger spatial scale, the dominant feature of the Greenland-only rebound predicted by Huy2 is a bulls-eye in uplift that is centred in central west Greenland, focussed between Nuuk and Sisimiut (Figure 2). The influence of this uplift centre extends northwards as far as Disko Bugt and to the south it influences all of the RSL sites considered here, although it diminishes in amplitude towards the southern tip of Greenland. Greenland-only uplift in the extreme south of the ice sheet (at Nanortalik) is predicted to be c. 20 m at 6 cal. ka BP (Simpson et al., 2009). Likewise, a strong Greenland rebound in response to retreat due to the HTM retreat contributes significantly to the modelled mid Holocene RSL highstand at Paamiut (Figure 5B). This shows that the RSL history of the southern part of Greenland is sensitive to changes in ice sheet loading to the north. Indeed, a smaller than predicted mid Holocene retreat of the ice sheet in central west Greenland would potentially reduce the modelled mid Holocene RSL highstand at Paamiut and reduce (but not remove) the current mis-match between model predictions and RSL observations. This hypothesis was tested by reducing the strength of the HTM in the Huy2 model forcing (Fig. 5C). The results show that Holocene sea levels are progressively reduced as the forcing (and thus response) is diminished in amplitude, indicating that this is one possible way to improve the data-model fit during the Holocene. Note, however, that this change also results in significant decrease in the predicted marine limit and therefore deterioration in the data-model fit for earlier times.

A final observation is that Huy2 consistently over-estimates the current ice sheet elevation (and thickness) in the coastal mountains of south west Greenland (Simpson et al., 2009). In the Paamiut area this over-estimate is c. 600 m and arises because the model predicts ice extending beyond the present observed ice sheet margin. Simpson et al. (2009) explain that this is caused by the steep terrain at the edge of the ice sheet, coupled with the 20 km model grid size. We note this because it means that RSL predictions at Paamiut (and elsewhere along much of the southern ice sheet margin) will be affected, principally by having too much ice on them. The consequence of this at Paamiut will be an underprediction in the amplitude of RSL fall during the Holocene; correcting for this may improve the early Holocene data fit but it will also cause more rebound in the mid and late Holocene, which will worsen data fit further.

6.2.4 North American ice sheets

As demonstrated in previous studies, Holocene RSL changes in Greenland are also affected by the GIA response to both North American and (to a lesser extent) Fennoscandian deglaciation (Fleming and Lambeck 2004). The unloading of these ice complexes affect RSL in Greenland through the influence of gravitational changes and eustasy on the ocean surface and through vertical land motion associated with their respective peripheral bulges. The forebulge of North American ice extended across much of Greenland, causing tens of meters of subsidence in west and south Greenland that variably offset the Greenland-only rebound: at 10 cal. ka BP Simpson et al. (2009) predicts between 40-45 m of subsidence from non-Greenland sources, compared to only 10-20 m at 11.5 cal. ka BP by Fleming and Lambeck (2004)). At 6 cal. ka BP, Simpson et al. predict c. -20 m of non-Greenland subsidence, approximately equal in magnitude to Greenland-only rebound (Simpson et al., 2009). One obvious way to reduce the model / data misfit at Paamiut and elsewhere in south Greenland during the mid-Holocene would be to increase the subsidence caused by the Laurentide forebulge collapse. To illustrate the sensitivity of RSL at Paamiut to North American ice, the ice thickness was scaled uniformly by 110% and 90% of that in the ICE-5G model. The results show (Figure 6D) that there is a significant sensitivity of RSL at Paamiut to this amplitude ice model change. Not surprisingly, the larger North American ice sheet model produces lower RSL values due to the enhanced forebulge collapse.

Whilst none of the model changes/limitations considered above can, on their own, account for the data-model mismatch at Paamiut, the results shown in Figure 6 indicate possible revisions that would act to reduce the misfit. For example, an effective route to lower predicted RSL values in the Holocene is by choosing a reduced HTM forcing (or response to this forcing; Fig. 6C). However none of the sensitivity tests provide an obvious solution to achieve the rapid RSL fall in the early Holocene. If this were to be achieved by a rapid local mass loss around 11 cal. ka BP, this would act to increase RSL values in the Holocene (and thus worsen the model fits for this period). A more probable working hypothesis is a rapid thinning of adjacent North American ice between ~11 and 9 cal. ka BP. Given the sensitivity shown in Fig. 5D, this could provide the amplitude of fall required but would not have a detrimental effect on the model fit during the

Holocene. These two model revisions – a smaller HTM forcing (or smaller response to this forcing) as well as a large NAIS signal in the early Holocene – are being considered for the next iteration of the Huy2 model.

7. Implications for the history of the Qassimiut Lobe

There has been some discussion about whether the Qassimiut Lobe is more or less sensitive to temperature changes than the rest of the southern part of the ice sheet. The Lobe terminates on land in its southern part at altitudes of less than 500 m asl compared to other parts of southern Greenland where the ice sheet margin is at elevations over 1000 m. Letreguilly et al. (1991) note that the high parts of the southern sector are relatively insensitive to a 3°C warming (similar to that during the HTM reconstructed from Dye3 (Dahl-Jensen et al., 1998)) because of the high bedrock terrain and also potential increases in precipitation. Weidick et al. (2004) also note that once the ice sheet in this region retreated to the fjord heads, the scope for further mass loss by calving would have been reduced. In contrast to the high elevation areas, Letreguilly et al. (1991) suggest that the lower lying Qassimiut Lobe would be more sensitive to climate change, with a modelled retreat of 40 to 50 km behind its present margin under 3 degrees of warming. Khan et al. (2008) demonstrate that the inclusion of a neoglacial readvance of the Lobe of about 33 km is required to satisfy present day GPS observations of vertical motion with model predictions by ICE-5G, which did not previously contain a readvance of this Lobe.

The notion that the low lying Qassimiut Lobe is more climatically sensitive than other parts of the southern Ice Sheet (Weidick et al. 2004) is contradicted by other geological data. As noted above, threshold lake evidence (Larsen et al., 2011) suggests a more modest response than implied by Weidick (2004) and Khan's modelling exercise. Our new RSL data suggest that the RSL records from two sites that embrace the Qassimiut Lobe (Paamiut and Qaqortoq) are pretty similar (Figure 3), and do not differ dramatically from the RSL data from Nanortalik in the far south. This suggests that any local scale response of the low-lying parts of the Lobe was not sufficiently large to distort the regional scale patterns of RSL that must have been driven by the main LGM-Holocene Greenland and far-field ice sheet load changes.

8. Conclusions

The main conclusions of this paper are:

1. New RSL data from Paamiut show rapid fall from a marine limit of c. 52 m asl at or before c. 10.9 cal. ka BP to close to present by c. 9.5 cal. ka BP, at rates of up to c. 32 mm/yr, falling below present for the rest of the Holocene. The elevation of the RSL lowstand at Paamiut is not well constrained; our data

show it was at least below -3 m, but based on studies elsewhere in southern Greenland it is more likely that it was between -5 and -10 m.

2. The rapid RSL fall during the early Holocene seen at Paamiut matches the pattern seen at Qaqortoq, suggesting rapid, largely simultaneous ice retreat from the area surrounding the Qassimiut lobe at the start of the Holocene. This retreat occurred c. 2000 years after the initial deglaciation of the extreme southern tip of Greenland (Bennike and Björck, 2002).

3. Our new data suggest that much of the southern part of the ice sheet records a broadly similar RSL history that is distinct to that recorded further north along the west coast. The main drivers of millennial-scale RSL changes in south west Greenland are large-scale processes acting over the whole of the region, including the bulls eye of uplift centred in the west (Figure 2) and the influence of the collapse of the North American ice sheets. The effects of local loading and unloading are not dominant in the RSL records from this region.

4. Our findings are in broad agreement with the pattern of vertical land motion at 10 ka cal. BP predicted by the Huy2 model. This spatial variability contributes to the transition between Transitional Type I-II and Type I RSL curves north of Paamiut, but a lack of high quality RSL data over a 500 km stretch of coast north of Paamiut makes delimiting this zone of transition difficult.

5. A regional GIA model by Sparrenbom (2006) tuned for the SW sector of Greenland with tightly prescribed ice margin and thickness data provides a good model/data fit but lacks a physically realistic, 3-D thermo-mechanical model of ice sheet evolution. In contrast, the Huy2 all-Greenland model, which includes a sophisticated ice model fails to satisfactorily predict the RSL histories at Paamiut, Qaqortoq or Nanortalik. Sensitivity tests indicate that the data-model misfits are most likely due to an over-estimate of the HTM forcing (or the response to this forcing) and error in the NAIS component of the background deglaciation model.

Acknowledgments

Fieldwork was completed by SAW and AJL, diatom analysis by SAW, dating sampling by SAW and AJL, with analyses by CLB. Ice sheet modelling was completed by GAM and BC. All authors contributed to writing of the paper. We thank Mike Kelly and Ole Bennike for advice on original radiocarbon datings in the Paamiut area. SAW and AJL thank Marie Johansen and Ortooraq Møller for assistance with field logistics in the Paamiut area. We also acknowledge assistance from the NERC radiocarbon facility, under allocation number 1505.0910. This paper is a contribution to PALSEA2, APEX, IGCP 588 and the INQUA Commission on Coastal and Marine Processes.

Table and Figure captions

Table 1. New and existing radiocarbon dates from the study area. The reference water level is based on an interpretation of the lithology and the diatom assemblage at each dated sample. Errors in RSL refer to the range of the indicative meaning of each isolation contact and field measurement errors. [1] Height revised from 42 - 52 m in Weidick et al., 2004, [2] Height revised from 33-44 m in Weidick et al., 2004, [3] Height revised from 21-35.5 m in Weidick et al., 2004 (see text for details), [4] Assume MTL as reference water level.

Figure 1. A) Map of Greenland showing the study location and others mentioned in the text. The numbers refer to the timing of local, coastal deglaciation in thousands of years BP from the Qaqortoq, Nanortalik, Paamiut and Nuuk areas. B) Map of the Paamiut area showing the location of previously studied isolation basins and those investigated in this study. C) Isolation basins, lakes and tidal ponds cored as part of this study. The number refers to their altitudes in metres above MTL.

Figure 2. Spatial plot of RSL predictions from the Huy2 model showing the vertical land motion component at 10 cal. ka BP for Greenland ice only (from Simpson et al., 2009).

Figure 3. Existing relative sea-level data from isolation basins at Sisimiut, Paamiut, Qaqortoq and Nanortalik in southern and south west Greenland with RSL predictions for each location from the Huy2 model (Simpson et al. 2009) using their preferred earth model, with a 120 km thick lithosphere, upper mantle viscosity of 5×10^{20} PaS and a lower mantle viscosity of 10^{21} Pas.

Figure 4. Summary diagrams showing the transition between marine and freshwater diatoms across the isolation and ingression contacts in the studied basins. Lake numbers refer to their height to the nearest metre asl. The bars refer to % of each summary diatom class in each sample. Polyhalobian and mesohalobian classes are marine and brackish species, oligohalobian-indifferent and halophobous are freshwater classes. The stratigraphy is summarised as grey – marine silts and clays, brown – gyttja, either laminated silt gyttja across the isolation/ingression contact or organic gyttja above the contact. We do not differentiate between laminated silt gyttja and organic gyttja in these diagrams. The contact between grey and brown on each diagram refers to the first occurrence of gyttja, which does not necessarily coincide with the quantified diatomological isolation contact between MHWST and HAT.

Figure 5. A) New RSL data from isolation basins cored in this study. The elevation of the marine limit is shown by a cross (the upper and lower limit depict the error band on the marine limit observations). A

minimum age for the marine limit is given from the onset of organic accumulation in lake P62 (radiocarbon dating error terms shown as the younger and older end of the band). B) Relative sea-level data from previous studies in the Paamiut area (open triangles) and from the current study (black triangles). All available data on the local marine limit is shown by crosses, again showing their errors. The model prediction (solid black line) is from the Huy2 model (Simpson et al., 2009) using their preferred earth model, with a 120 km thick lithosphere, upper mantle viscosity of 5 x 10^{20} PaS and a lower mantle viscosity of 10^{22} Pas. The model prediction (dashed line) is from Sparrenbom 2006 and uses a lithospheric thickness of 50 km, upper mantle viscosity of 4 x 10^{20} PaS and a lower mantle viscosity of 10^{22} Pas.

Figure 6. Model results that show the sensitivity of RSL at Paamiut for different parameter sets. In all cases, the solid black line shows the prediction for the Huy2 ice model and the Earth viscosity model with a lithospheric thickness of 96 km, upper mantle viscosity of 5×10^{20} Pas and lower mantle viscosity of 10^{22} Pas. This model is within the subset of 8 (out of ~300) that produced an optimal fit to the Greenland-wide RSL data set considered in Simpson et al. (2009). (A) Sensitivity to changes in the adopted Earth viscosity model. Values refer to lithosphere thickness, upper mantle and lower mantle viscosity in turn (B) Sensitivity to changes in the timing of margin retreat from the continental shelf to the present day coast and the magnitude of a Younger Dryas readvance in south Greenland (C) Sensitivity to the strength of the Holocene Thermal Maximum, scaled compared to that in the Huy2 model (D) Sensitivity to scaling the heights of the North American ice sheets compared to the ICE-5G model.

Figures A1-9. Diatom diagrams from the sample cores. Frequencies are expressed as a percentage of total diatom valves and taxa are grouped according to the halobian classification scheme. Only species that equal or exceed 5 % of the total diatom valves are shown in each diagram. The core stratigraphies are summarised in the same way as in Figure 4 of the main paper.

References

Anderson, N.J., Bennike, O., Christoffersen, K., Jeppesen, E., Markager, S., Miller, G., Renberg, I., 1999. Limnological studies of lakes in south-western Greenland. Geology of Greenland Survey Bulletin 183, 68-74.

Bennike, O., Björck, S., 2002. Chronology of the last recession of the Greenland Ice Sheet. Journal of Quaternary Science 17, 211-219.

Björck, S., Bennike, O., Rosen, P., Andresen, C.S., Bohncke, S., Kaas, E., Conley, D., 2002. Anomalously mild Younger Dryas summer conditions in southern Greenland. Geology 30, 427-430.

Bronk Ramsey, C., 2009. Bayesian analysis of radiocarbon dates. Radiocarbon 51, 337-360.

Carlson, A., Stoner, J.S., Donnelly, J.P., Hillaire-Marcel, C., 2008. Response of the southern Greenland Ice Sheet during the last two deglaciations. Geology 36, 359-362.

Clark, J.A., Farrell, W.E., Peltier, W.R., 1978. Global changes in post glacial sea-level: a numerical equation. Quaternary Research 9, 265-287.

Dahl-Jensen, D., Mosegaard, K., Gundestrup, N., Clow, G.D., Johnsen, S.J., Hansen, A.W., Balling, N., 1998. Past temperatures directly from the Greenland Ice Sheet. Science 282, 268-271.

Fleming, K., Lambeck, K., 2004. Constraints on the Greenland Ice Sheet since the Last Glacial Maximum from sea-level observations and glacial-rebound models. Quaternary Sci Rev 23, 1053-1077.

Funder, S., Kjeldsen, K.K., Kjaer, K.H., O Cofaigh, C., 2011. The Greenland Ice Sheet during the last 300,000 years: a review, Developments in Quaternary Science. Elsevier, pp. 699-713. doi: 610.1016/B1978-1010-1444-53447-53447.00050-53447.

Kaplan, M.R., Wolfe, A.P., Miller, G.H., 2002. Holocene environmental variability in southern Greenland inferred from lake sediments. Quaternary Research 58, 149-159.

Kelly, M., 1980. The status of the Neoglacial in Western Greenland. Rapport Grønlands Geologiske Undersøgelse 96, 1-24.

Kelly, M., Funder, S., 1974. The pollen stratigraphy of late Quaternary lake sediments in Southern West Greenland. Rapport Grønlands Geologiske Undersøgelse 64, 26 pp.

Khan, S.A., Wahr, J., Leuliette, E., van Dam, T., Larson, K.M., Francis, O., 2008. Geodetic measurements of postglacial adjustments in Greenland. Journal of Geophysical Research-Solid Earth 113, B02402.

Knutz, P.C., Sicre, M.A., Ebbesen, H., Christiansen, S., Kuijpers, A., 2011. Multiple-stage deglacial retreat of the southern Greenland Ice Sheet linked with Irminger Current warm water transport. Paleoceanography 26, Doi 10.1029/2010pa002053.

Larsen, N.K., Funder, S., Kjaer, K.H., Kjeldsen, K.K., Knudsen, M.F., Linge, H., In press. Rapid early Holocene ice retreat in West Greenland. Quaternary Sci Rev.

Larsen, N.K., Kjaer, K.H., Olsen, J., Funder, S., Kjeldsen, K.K., Norgaard-Pedersen, N., 2011. Restricted impact of Holocene climate variations on the southern Greenland Ice Sheet. Quaternary Sci Rev 30, 3171-3180.

Letreguilly, A., Huybrechts, P., Reeh, N., 1991. Steady-State Characteristics of the Greenland Ice-Sheet under Different Climates. J Glaciol 37, 149-157.

Long, A.J., Roberts, D.H., Dawson, S., 2006. Early Holocene history of the West Greenland Ice Sheet and the GH-8.2 event. Quaternary Sci Rev 25, 904-922.

Long, A.J., Roberts, D.H., Wright, M.R., 1999. Isolation basin stratigraphy and Holocene relative sea-level change on Arveprinsen Ejland, Disko Bugt, West Greenland. Journal of Quaternary Science 14, 323-345.

Long, A.J., Woodroffe, S.A., Dawson, S., Roberts, D.H., Bryant, C.L., 2009. Late Holocene relative sea-level rise and the Neoglacial history of the Greenland ice sheet. Journal of Quaternary Science 24, 345-359.

Long, A.J., Woodroffe, S.A., Roberts, D.H., Dawson, S., 2011. Isolation basins, sea-level changes and the Holocene history of the Greenland Ice Sheet. Quaternary Sci Rev 30, 3748-3768.

Massa, C., Perren, B.B., Gauthier, E., Bichet, V., Petit, C., Richard, H., 2012. A multiproxy evaluation of Holocene environmental change from Lake Igaliku, South Greenland. J Paleolimnol 48, 241-258.

Reimer, P.J., Baillie, M.G.L., Bard, E., Bayliss, A., Beck, J.W., Blackwell, P.G., Ramsey, C.B., Buck, C.E., Burr, G.S., Edwards, R.L., Friedrich, M., Grootes, P.M., Guilderson, T.P., Hajdas, I., Heaton, T.J., Hogg, A.G., Hughen, K.A., Kaiser, K.F., Kromer, B., McCormac, F.G., Manning, S.W., Reimer, R.W., Richards, D.A., Southon, J.R., Talamo, S., Turney, C.S.M., van der Plicht, J., Weyhenmeye, C.E., 2009. Intcal09 and Marine09 Radiocarbon Age Calibration Curves, 0-50,000 Years Cal BP. Radiocarbon 51, 1111-1150.

Simpson, M.J.R., Milne, G.A., Huybrechts, P., Long, A.J., 2009. Calibrating a glaciological model of the Greenland ice sheet from the last glacial maximum to present-day using field observations of relative sea level and ice extent. Quaternary Sci Rev 28, 1631-1657.

Simpson, M.J.R., Wake, L., Milne, G.A., Huybrechts, P., 2011. The influence of decadal- to millennial-scale ice mass changes on present-day vertical land motion in Greenland: Implications for the interpretation of GPS observations. Journal of Geophysical Research-Solid Earth 116, B02406.

Sparrenbom, C.J., 2006. Constraining the southern part of the Greenland Ice Sheet since the Last Glacial Maximum from relative sea-level changes, cosmogenic dates and glacial-isostatic adjustment models Department of Geology. Lund University, Lund, p. 125 p.

Sparrenbom, C.J., Bennike, O., Björck, S., Lambeck, K., 2006a. Holocene relative sea-level changes in the Qaqortoq area, southern Greenland. Boreas 35, 171-187.

Sparrenbom, C.J., Bennike, O., Björck, S., Lambeck, K., 2006b. Relative sea-level changes since 15 000 cal. yr BP in the Nanortalik area, Southern Greenland. Journal of Quaternary Science 21, 29-48.

Tarasov, L., Peltier, W.R., 2002. Greenland glacial history and local geodynamic consequences. Geophysical Journal International 150, 198-229.

Tauber, H., 1968. Copenhagen radiocarbon dates IX. Radiocarbon 10, 295-327.

Weidick, A., Kelly, M., Bennike, O., 2004. Late Quaternary development of the southern sector of the Greenland Ice Sheet, with particular reference to the Qassimiut lobe. Boreas 33, 284-299.

Whitehouse, P.L., Bentley, M.J., Milne, G.A., King, M.A., Thomas, I.D., 2012. A new glacial isostatic adjustment model for Antarctica: calibrated and tested using observations of relative sea-level change and present-day uplift rates. Geophysical Journal International in press.

Basin	Mid sill height (m MTL)	Reference water level	RSL (m MTL)	^{14}C age (± 1 σ)	Material dated	Lab code	Max age (cal yr BP) (± 2 σ)	Min age (cal yr BP) (± 2 σ)	Mid age (cal yr BP)
P62 (this study)	62	Above marine limit (51.7-53.4 m asl)	52.55 ± 0.95	9154 ± 41	Bulk gyttja	SUERC-34122	10480	10231	10355
P38 (this study)	38.82	Isolation (MHWST to HAT)	37.23 ± 0.12	9673 ± 40	Bulk gyttja	SUERC-34121	11206	10800	11003
P24 (this study)	24.86	Isolation (MHWST to HAT)	23.27 ± 0.17	9027 ± 43	Bulk gyttja	SUERC-34126	10254	9963	10108
P12 (this study)	12.23	Isolation (MHWST to HAT)	10.64 ± 0.27	8630 ± 38	Bulk gyttja	SUERC-34123	9676	9533	9604
P2 (this study)	1.99	Isolation (MHWST to HAT)	0.4 ± 0.18	8451 ± 40	Bulk gyttja	SUERC-34115	9534	9423	9478
P0 (this study)	0.64	Isolation (MHWST to HAT)	-0.95 ± 0.15	8339 ± 40	Bulk gyttja	SUERC-34116	9470	9258	9364
P-1 (this study)	-1.07	Isolation (MHWST to HAT)	-2.66 ± 0.21	8539 ± 37	Bulk gyttja	SUERC-34124	9548	9482	9515
P-1 (this study)	-1.07	Ingression (MHWST to HAT)	-2.66 ± 0.21	941 ± 37	Bulk gyttja	SUERC-34125	931	776	853
P0 (this study)	0.64	Ingression (HAT)	-1.14 ± 0.15	1439 ± 37	Bulk gyttja	SUERC-34118	1393	1292	1342
P0 (this study)	0.64	Freshwater limiting	below -1.14 ± 0.15	2268 ± 37	Bulk gyttja	SUERC-34117	2349	2156	2252
Qaqarsuaq (Tauber 1968)[1]	52	Isolation (HAT)	50.22 ± 2	9840 ± 170	Bulk gyttja	K-1149	11964	10745	11354
Qaqarsuaq (Tauber 1968)[2]	44	Isolation (HAT)	42.22 ± 2	8510 ± 160	Bulk gyttja	K-1150	10119	9033	9576
Qaqarsuaq (Tauber 1968)[3]	35.5	Isolation (HAT)	33.72 ± 2	8680 ± 160	Bulk gyttja	K-1151	10190	9439	9814
Qivdlagissat (Tauber 1968)	22	Isolation (HAT)	20.22 ± 2	7750 ± 150	Bulk gyttja	K-1153	9006	8223	8614
Sarfa (Tauber 1968)	4	Isolation (HAT)	2.22 ± 2	4780 ± 120	Bulk gyttja	K-1152	5883	5076	5479
Paamiut 2 (Anderson et al., 1999)[4]	17	Isolation (MTL)	17 ± 2	8800	Bulk gyttja	Not known	9902	9742	9822
Nigerleq (Kelly & Funder 1974)	90	Above marine limit	52.55 ± 0.85	9580 ± 210	Bulk gyttja	K-988	11594	10251	10922
Paamiut 1 (Anderson et al., 1999)	Not known	Above marine limit	52.55 ± 0.85	9600	Bulk gyttja	Not known	11099	10790	10944

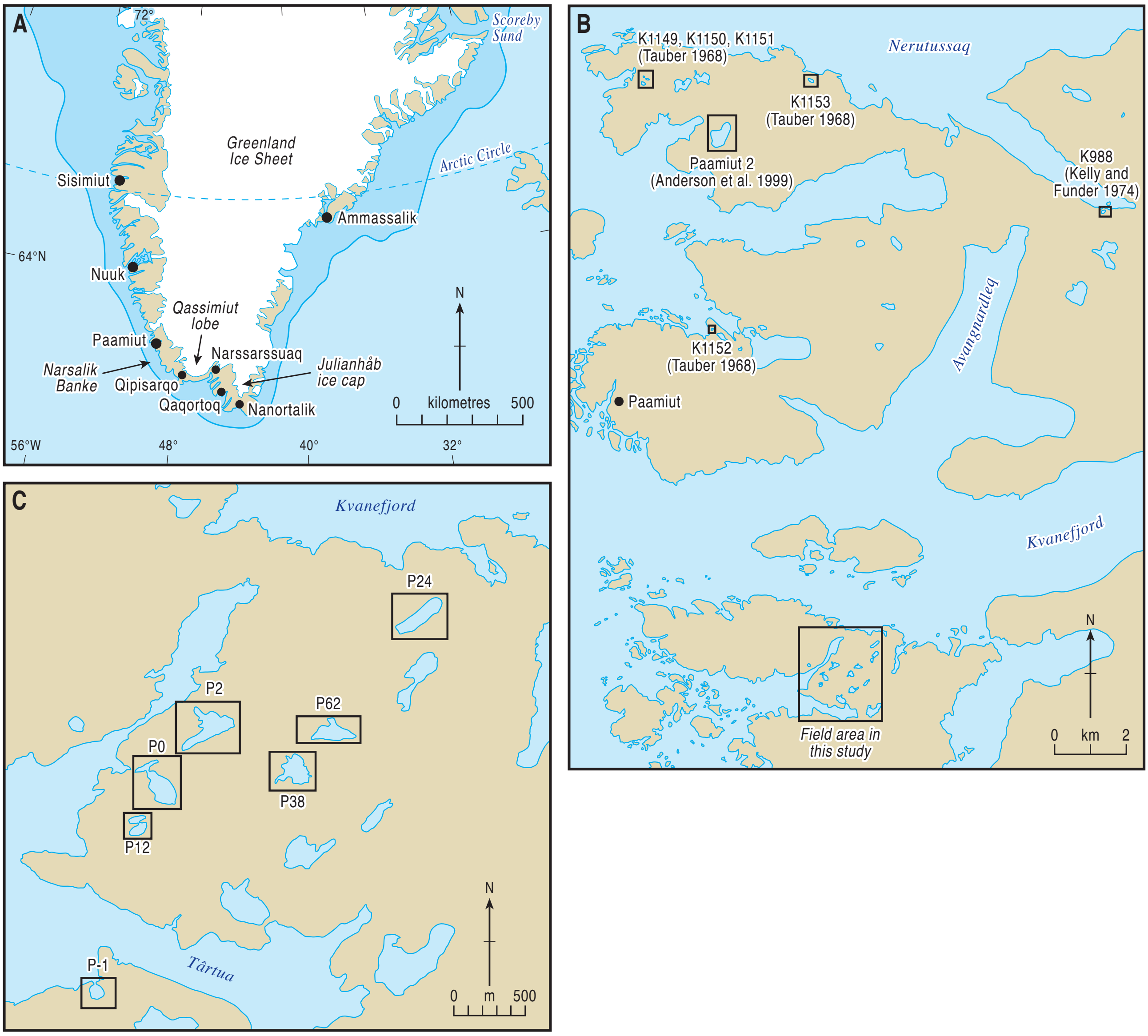

A
72°
Scoreby Sund
Greenland Ice Sheet
Arctic Circle
Sisimiut
Ammassalik
64°N
Nuuk
Qassimiut lobe
Paamiut
Narssarssuaq
Julianhåb ice cap
Narsalik Banke
Qipisarqo
Qaqortoq
Nanortalik
N
0 kilometres 500
56°W
48°
40°
32°
B
K1149, K1150, K1151 (Tauber 1968)
Nerutussaq
K1153 (Tauber 1968)
Paamiut 2 (Anderson et al. 1999)
K988 (Kelly and Funder 1974)
Avangnardleq
K1152 (Tauber 1968)
Paamiut
Kvanefjord
N
Field area in this study
0 km 2
C
Kvanefjord
P24
P2
P62
P0
P38
P12
N
Târtua
P-1
0 m 500

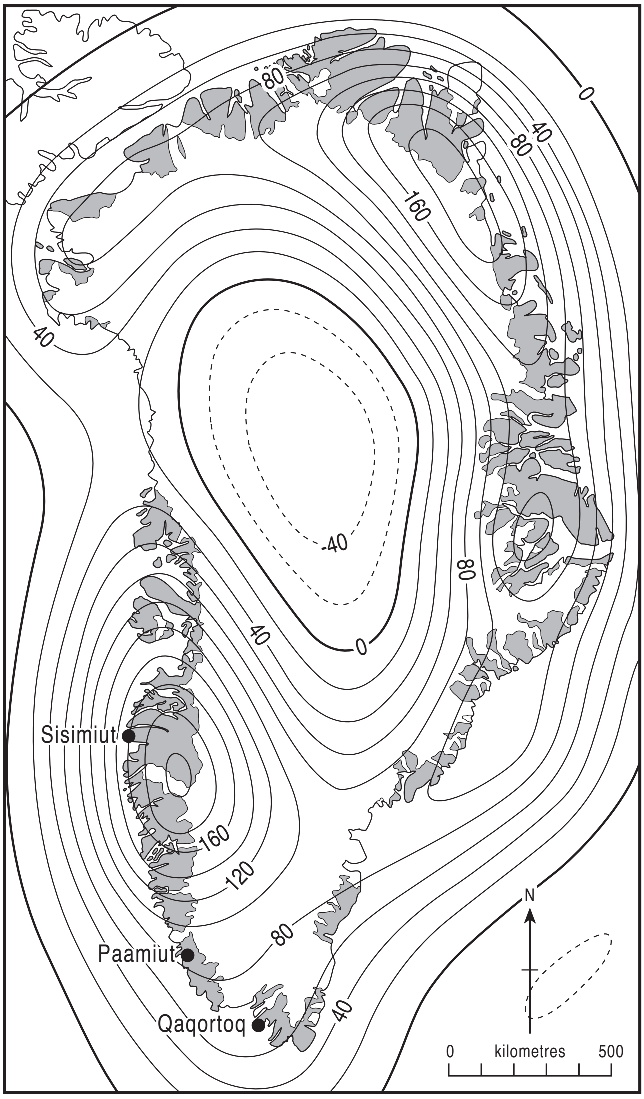

0
40
80
80
40
160
80
-40
0
40
Sisimiut
160
120
80
Paamiut
Qaqortoq
40
N
0
kilometres
500

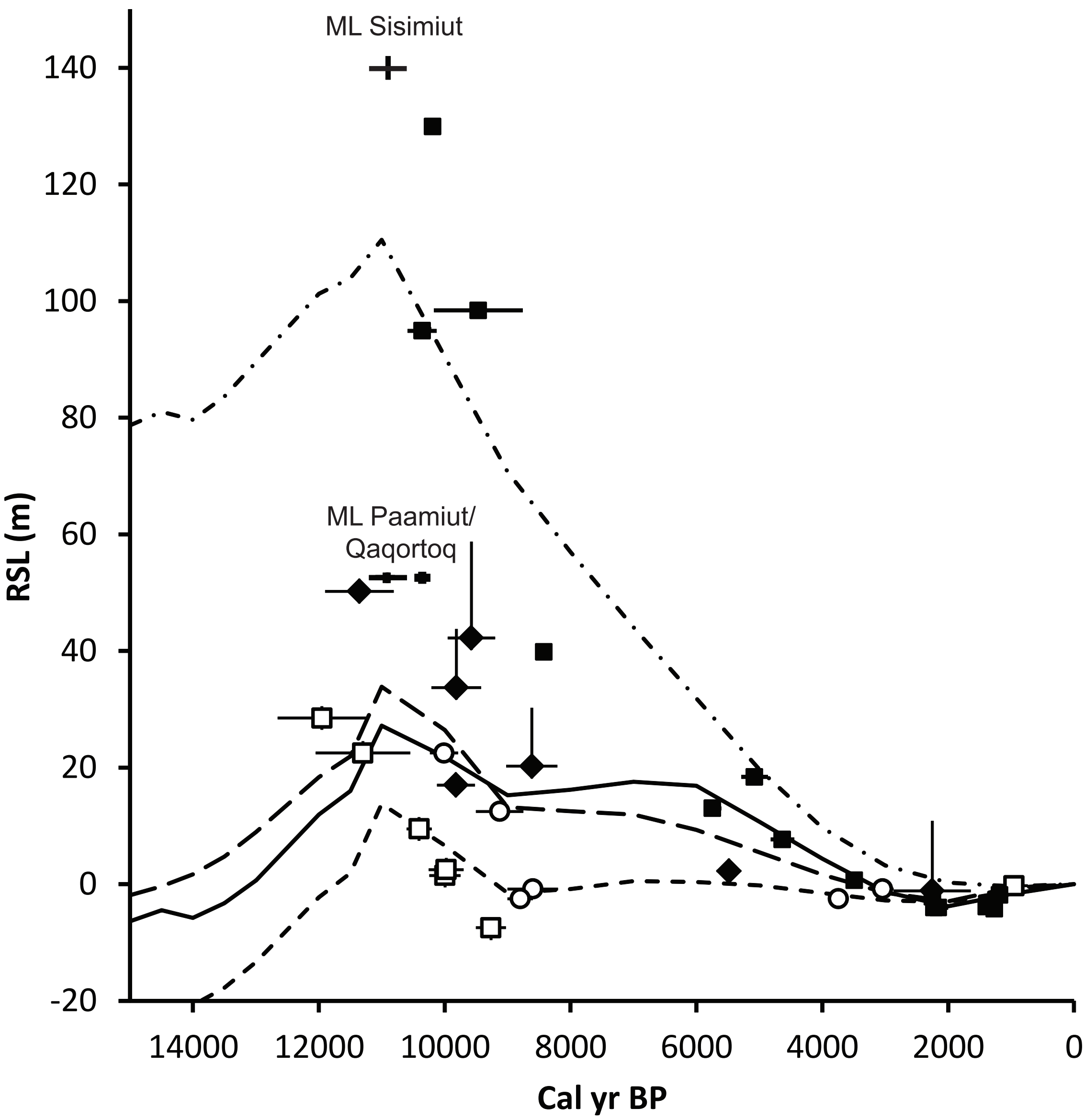

■ Sisimiut (Long et al., 2009; Bennike et al., 2011)
◆ Paamiut (Tauber 1968, Kelly and Funder 1974, Anderson et al., 1999)
○ Outer coast near Qaqortoq (Sparrenbom et al., 2006a)
□ Sites near Nanortalik (Sparrenbom et al., 2006b)
ML = Marine limit

Huy2 model predictions for:
Sisimiut
Paamiut
Qaqortoq
Nanortalik

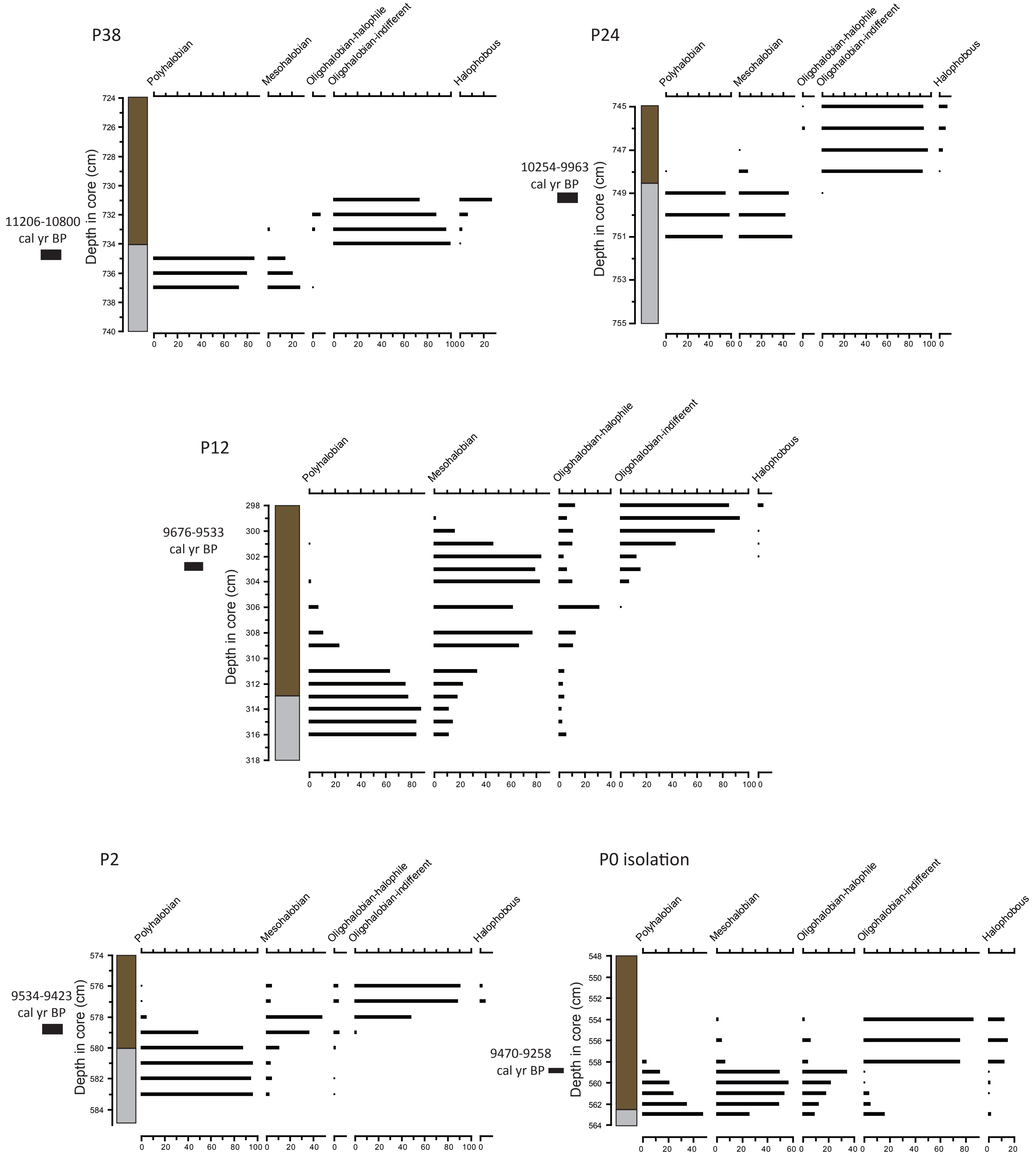

P38
Polyhalobian
Mesohalobian
Oligohalobian-halophile
Oligohalobian-indifferent
Halophobous
Depth in core (cm)
11206-10800
cal yr BP
P24
10254-9963
cal yr BP
P12
9676-9533
cal yr BP
P2
9534-9423
cal yr BP
P0 isolation
9470-9258
cal yr BP

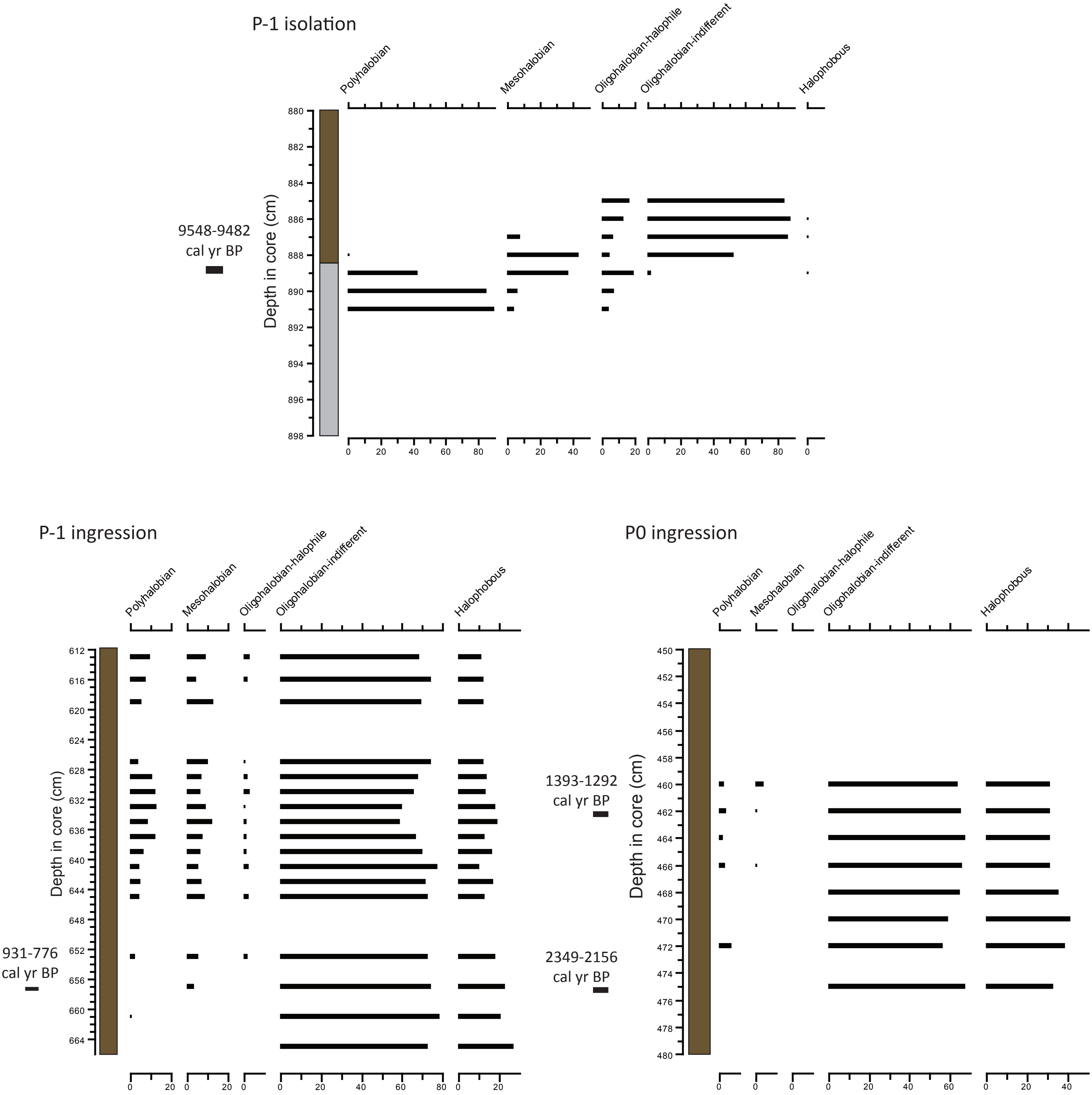
P-1 isolation
Polyhalobian
Mesohalobian
Oligohalobian-halophile
Oligohalobian-indifferent
Halophobous
Depth in core (cm)
9548-9482
cal yr BP
880
882
884
886
888
890
892
894
896
898
0 20 40 60 80
0 20 40
0 20
0 20 40 60 80
0
P-1 ingression
Polyhalobian
Mesohalobian
Oligohalobian-halophile
Oligohalobian-indifferent
Halophobous
Depth in core (cm)
931-776
cal yr BP
612
616
620
624
628
632
636
640
644
648
652
656
660
664
0 20
0 20
0
0 20 40 60 80
0 20
P0 ingression
Polyhalobian
Mesohalobian
Oligohalobian-halophile
Oligohalobian-indifferent
Halophobous
Depth in core (cm)
1393-1292
cal yr BP
2349-2156
cal yr BP
450
452
454
456
458
460
462
464
466
468
470
472
474
476
478
480
0
0
0
0 20 40 60
0 20 40

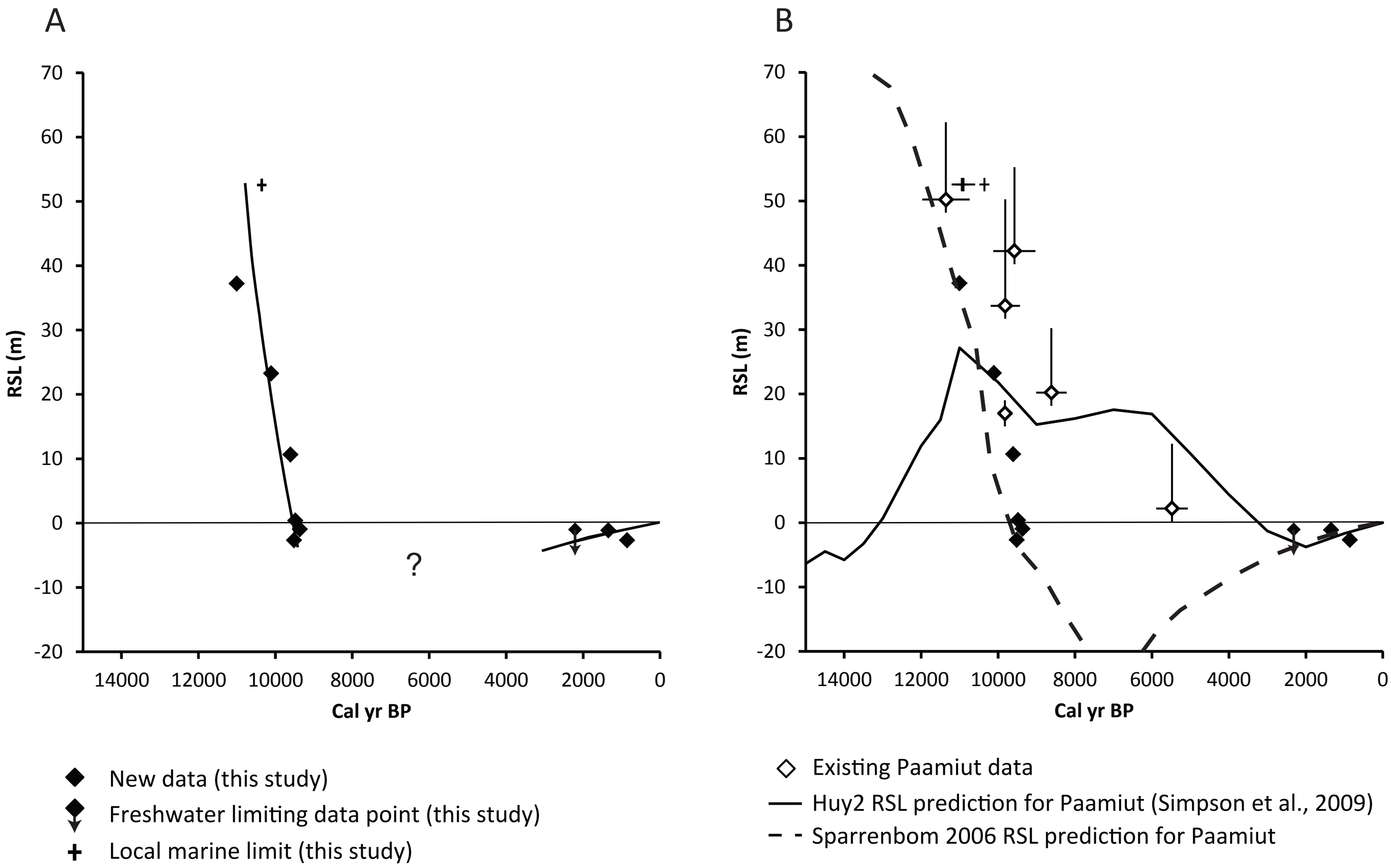

A
B
70
60
50
40
30
20
10
0
-10
-20
RSL (m)
14000
12000
10000
8000
6000
4000
2000
0
Cal yr BP
?
New data (this study)
Freshwater limiting data point (this study)
Local marine limit (this study)
Existing Paamiut data
Huy2 RSL prediction for Paamiut (Simpson et al., 2009)
Sparrenbom 2006 RSL prediction for Paamiut

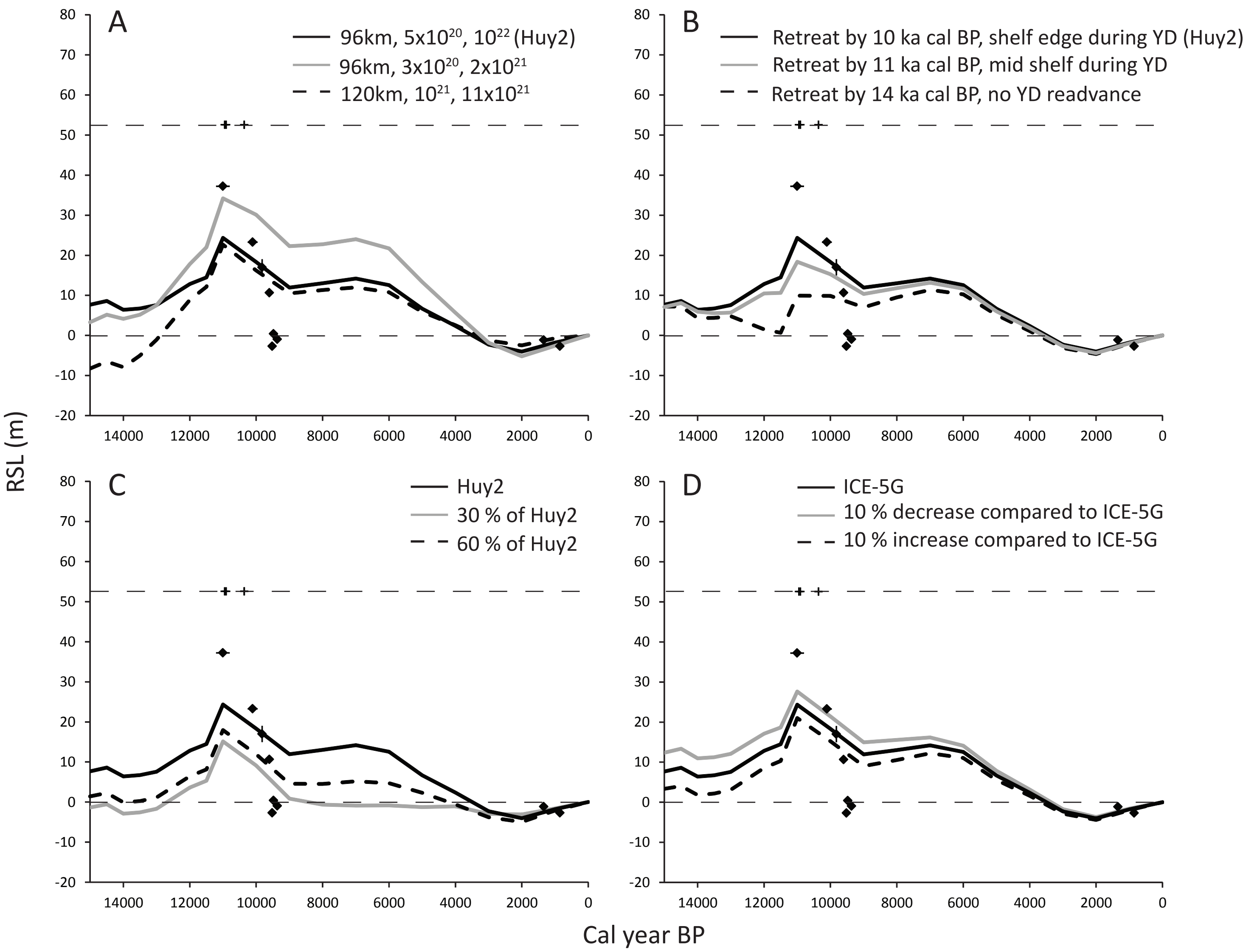
A
96km, 5x10[20], 10[22] (Huy2)
96km, 3x10[20], 2x10[21]
120km, 10[21], 11x10[21]
B
Retreat by 10 ka cal BP, shelf edge during YD (Huy2)
Retreat by 11 ka cal BP, mid shelf during YD
Retreat by 14 ka cal BP, no YD readvance
C
Huy2
30 % of Huy2
60 % of Huy2
D
ICE-5G
10 % decrease compared to ICE-5G
10 % increase compared to ICE-5G
RSL (m)
Cal year BP

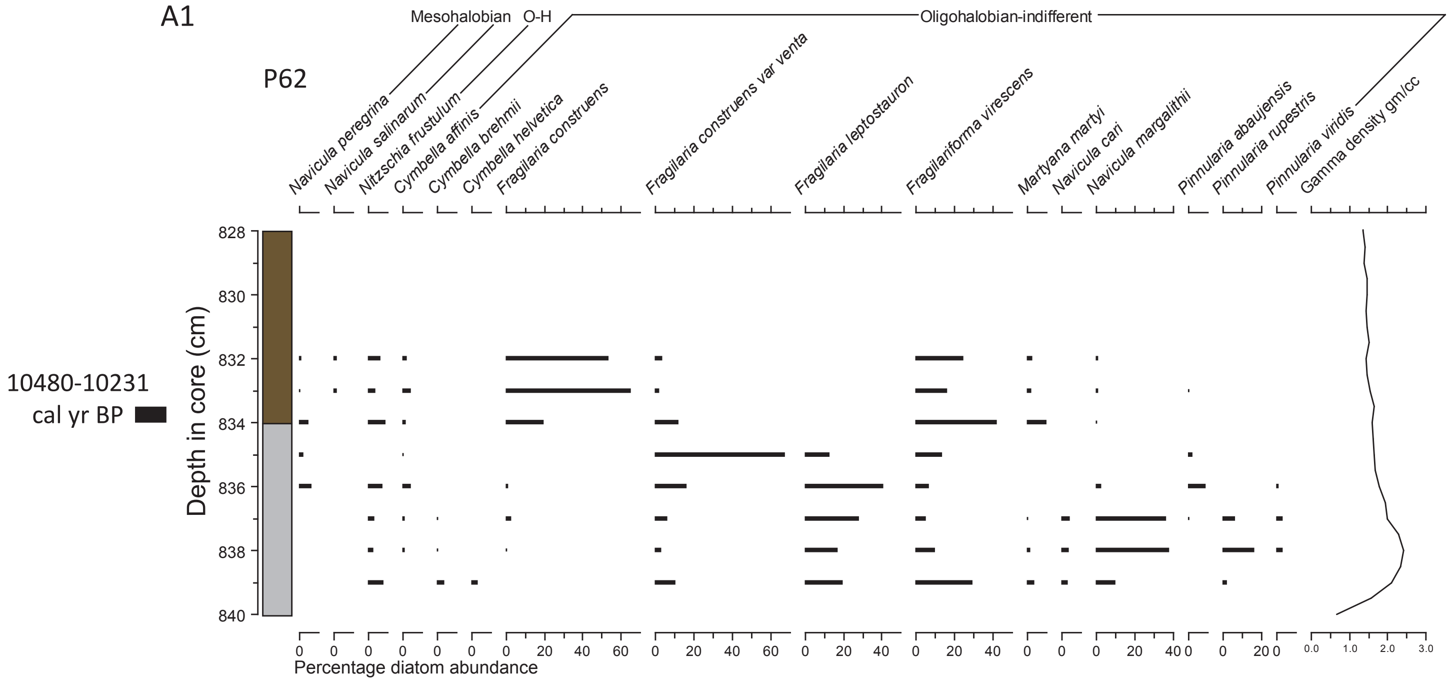
A1
P62
Mesohalobian
O-H
Oligohalobian-indifferent
Navicula peregrina
Navicula salinarum
Nitzschia frustulum
Cymbella affinis
Cymbella brehmii
Cymbella helvetica
Fragilaria construens
Fragilaria construens var venta
Fragilaria leptostauron
Fragilariforma virescens
Martyana martyi
Navicula cari
Navicula margalithii
Pinnularia abaujensis
Pinnularia rupestris
Pinnularia viridis
Gamma density gm/cc
Depth in core (cm)
10480-10231
cal yr BP
Percentage diatom abundance

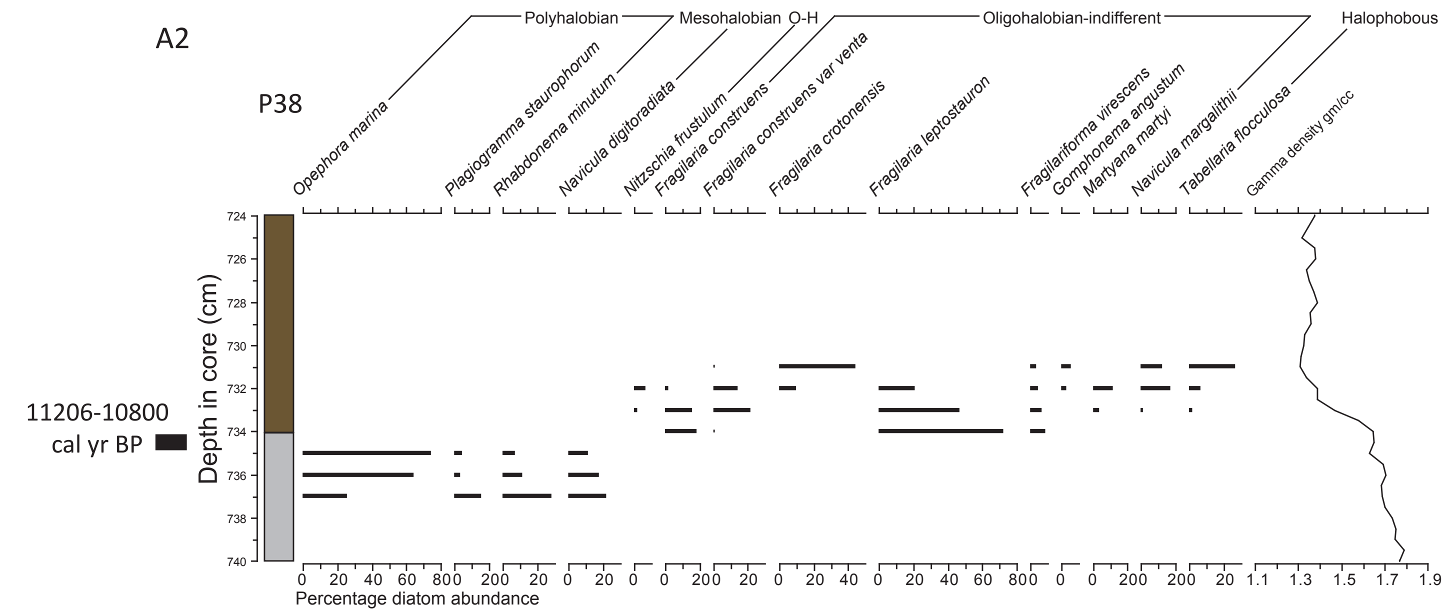
A2
P38
Polyhalobian
Mesohalobian
O-H
Oligohalobian-indifferent
Halophobous
Opephora marina
Plagiogramma staurophorum
Rhabdonema minutum
Navicula digitoradiata
Nitzschia frustulum
Fragilaria construens
Fragilaria construens var venta
Fragilaria crotonensis
Fragilaria leptostauron
Fragilariforma virescens
Gomphonema angustum
Martyana martyi
Navicula margalithii
Tabellaria flocculosa
Gamma density gm/cc
Depth in core (cm)
11206-10800
cal yr BP
Percentage diatom abundance

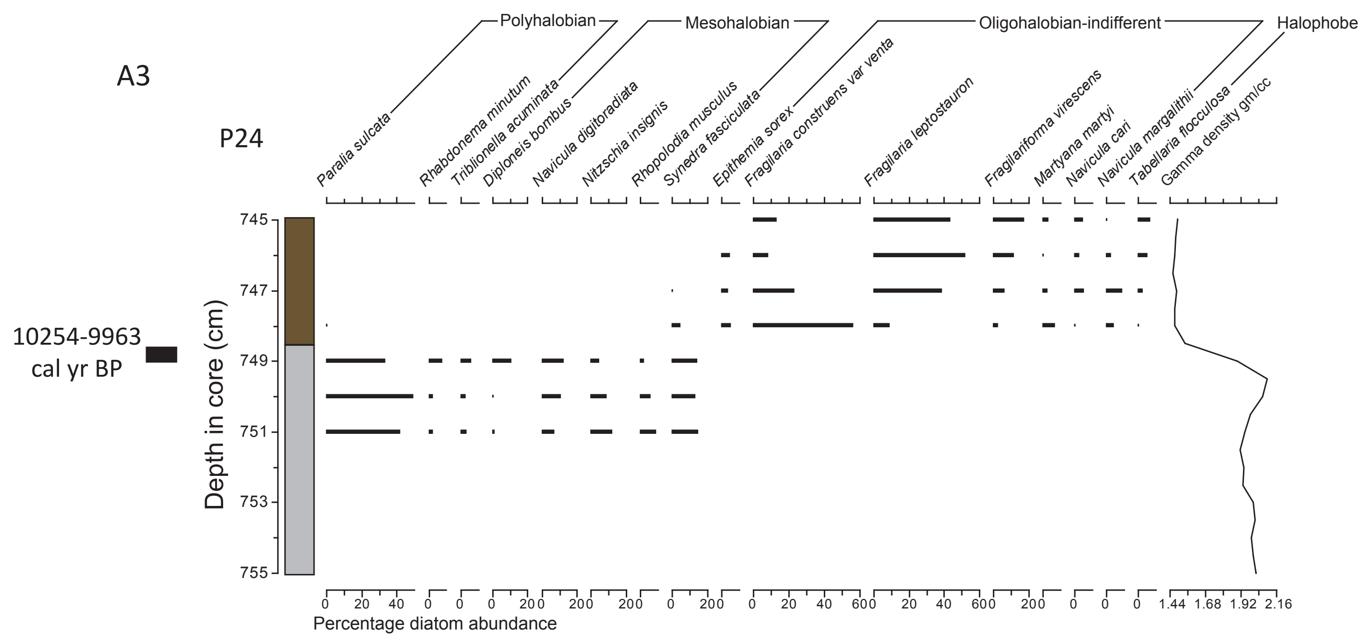
A3
P24
Polyhalobian
Mesohalobian
Oligohalobian-indifferent
Halophobe
Paralia sulcata
Rhabdonema minutum
Triblionella acuminata
Diploneis bombus
Navicula digitoradiata
Nitzschia insignis
Rhopolodia musculus
Synedra fasciculata
Epithemia sorex
Fragilaria construens var venta
Fragilaria leptostauron
Fragilariforma virescens
Martyana martyi
Navicula cari
Navicula margalithii
Tabellaria flocculosa
Gamma density gm/cc
Depth in core (cm)
10254-9963
cal yr BP
Percentage diatom abundance

A4

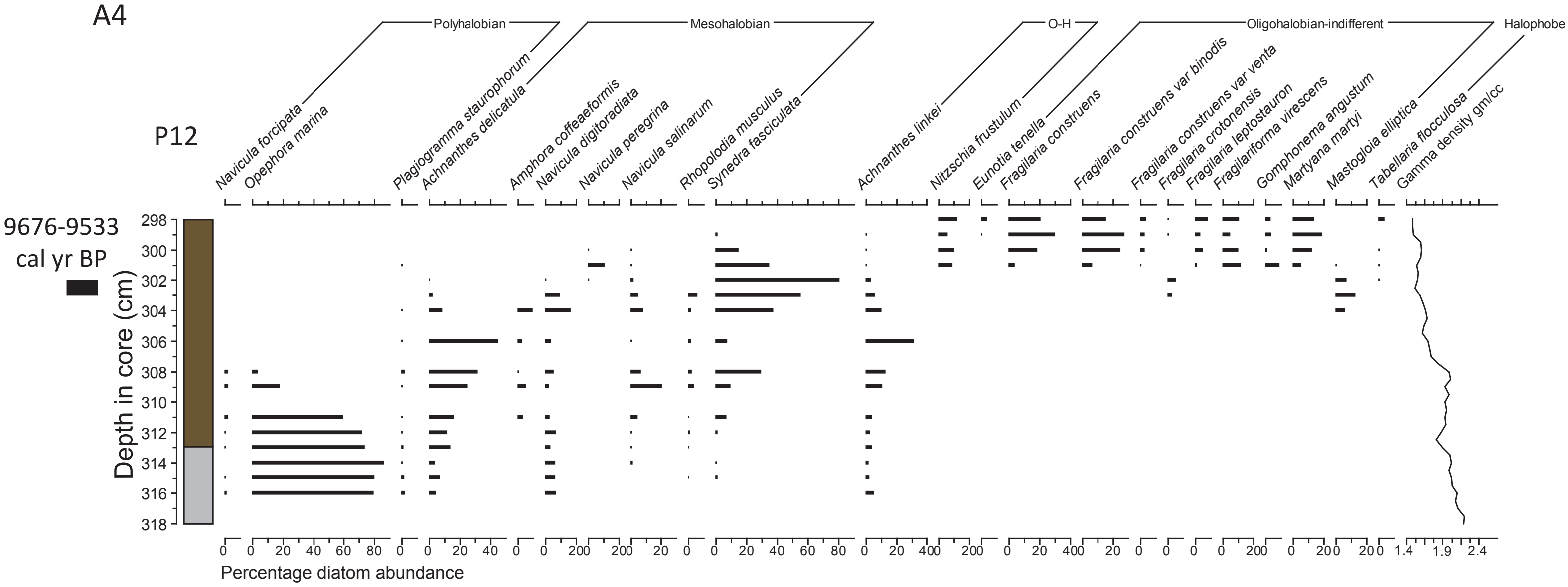
Polyhalobian
Mesohalobian
O-H
Oligohalobian-indifferent
Halophobe
P12
Navicula forcipata
Opephora marina
Plagiogramma staurophorum
Achnanthes delicatula
Amphora coffeaeformis
Navicula digitoradiata
Navicula peregrina
Navicula salinarum
Rhopolodia musculus
Synedra fasciculata
Achnanthes linkei
Nitzschia frustulum
Eunotia tenella
Fragilaria construens
Fragilaria construens var binodis
Fragilaria construens var venta
Fragilaria crotonensis
Fragilaria leptostauron
Fragilariforma virescens
Gomphonema angustum
Martyana martyi
Mastogloia elliptica
Tabellaria flocculosa
Gamma density gm/cc
9676-9533
cal yr BP
Depth in core (cm)
Percentage diatom abundance

A5

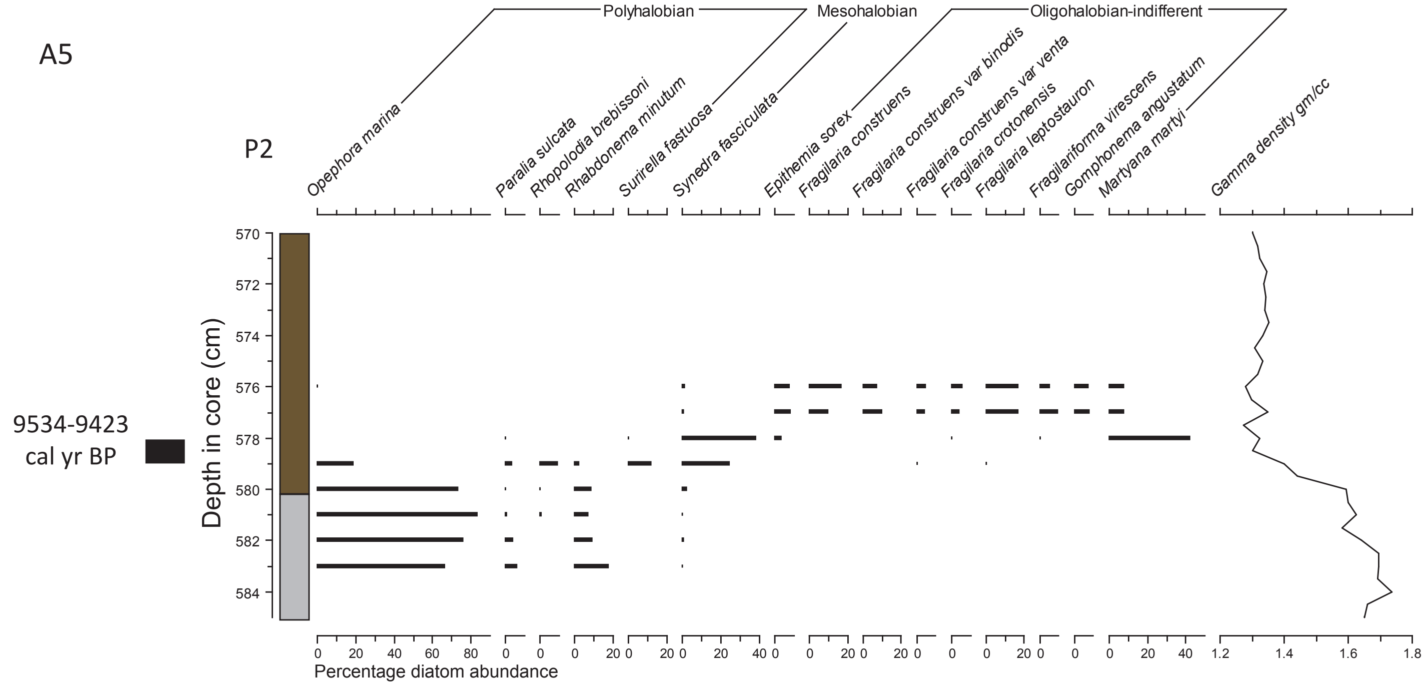
Polyhalobian
Mesohalobian
Oligohalobian-indifferent
P2
Opephora marina
Paralia sulcata
Rhopolodia brebissoni
Rhabdonema minutum
Surirella fastuosa
Synedra fasciculata
Epithemia sorex
Fragilaria construens
Fragilaria construens var binodis
Fragilaria construens var venta
Fragilaria crotonensis
Fragilaria leptostauron
Fragilariforma virescens
Gomphonema angustatum
Martyana martyi
Gamma density gm/cc
9534-9423
cal yr BP
Depth in core (cm)
Percentage diatom abundance

A6

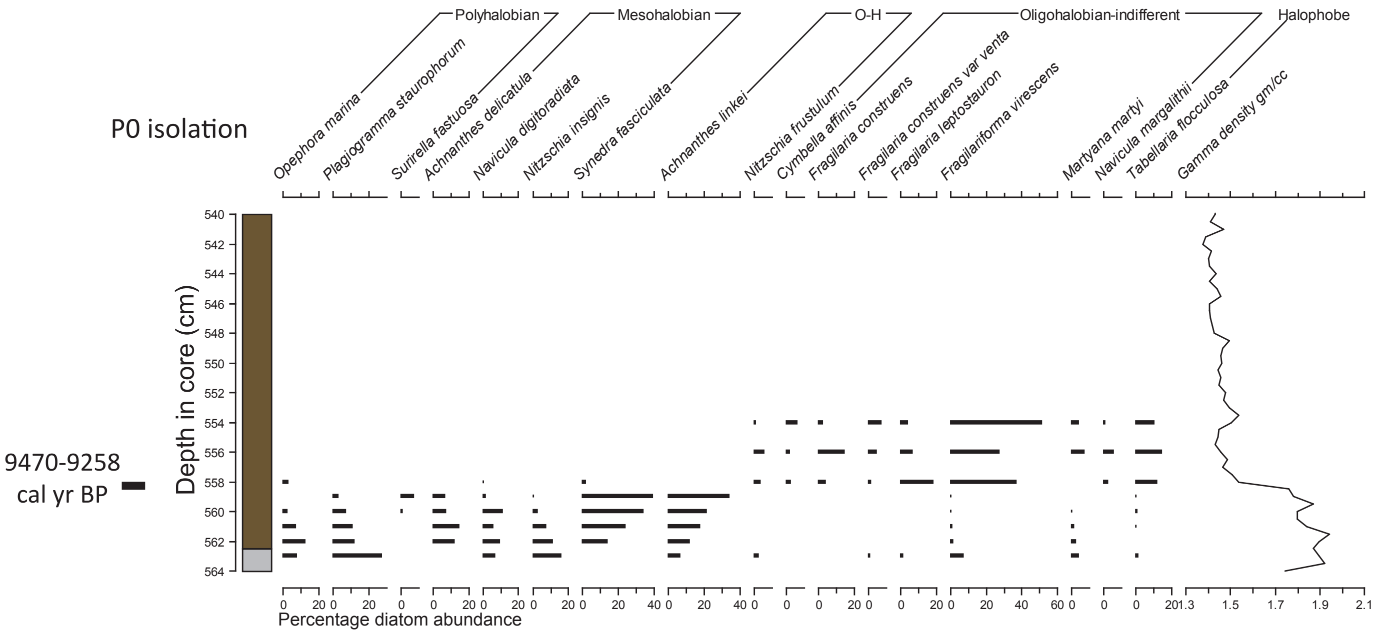
Polyhalobian
Mesohalobian
O-H
Oligohalobian-indifferent
Halophobe
P0 isolation
Opephora marina
Plagiogramma staurophorum
Surirella fastuosa
Achnanthes delicatula
Navicula digitoradiata
Nitzschia insignis
Synedra fasciculata
Achnanthes linkei
Nitzschia frustulum
Cymbella affinis
Fragilaria construens
Fragilaria construens var venta
Fragilaria leptostauron
Fragilariforma virescens
Martyana martyi
Navicula margalithii
Tabellaria flocculosa
Gamma density gm/cc
9470-9258
cal yr BP
Depth in core (cm)
Percentage diatom abundance

A7

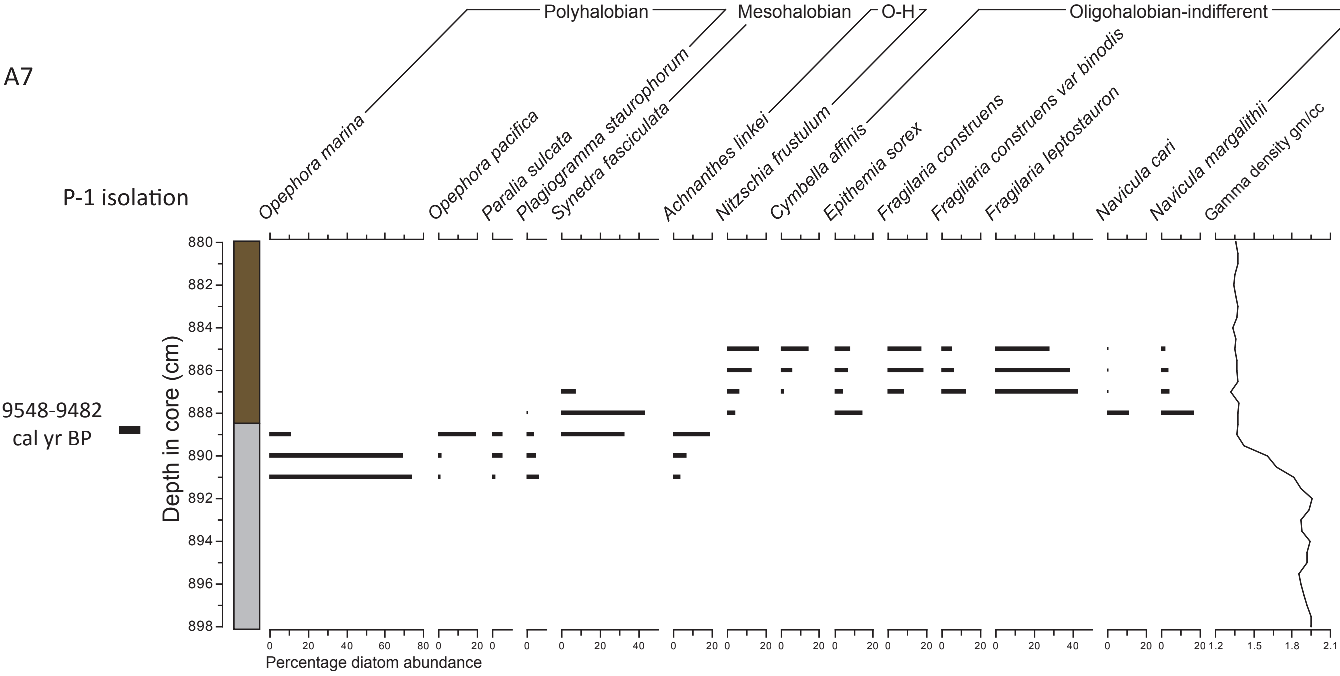

P-1 isolation
Polyhalobian
Mesohalobian
O-H
Oligohalobian-indifferent
Opephora marina
Opephora pacifica
Paralia sulcata
Plagiogramma staurophorum
Synedra fasciculata
Achnanthes linkei
Nitzschia frustulum
Cymbella affinis
Epithemia sorex
Fragilaria construens
Fragilaria construens var binodis
Fragilaria leptostauron
Navicula cari
Navicula margalithii
Gamma density gm/cc
Depth in core (cm)
9548-9482 cal yr BP
Percentage diatom abundance

A8

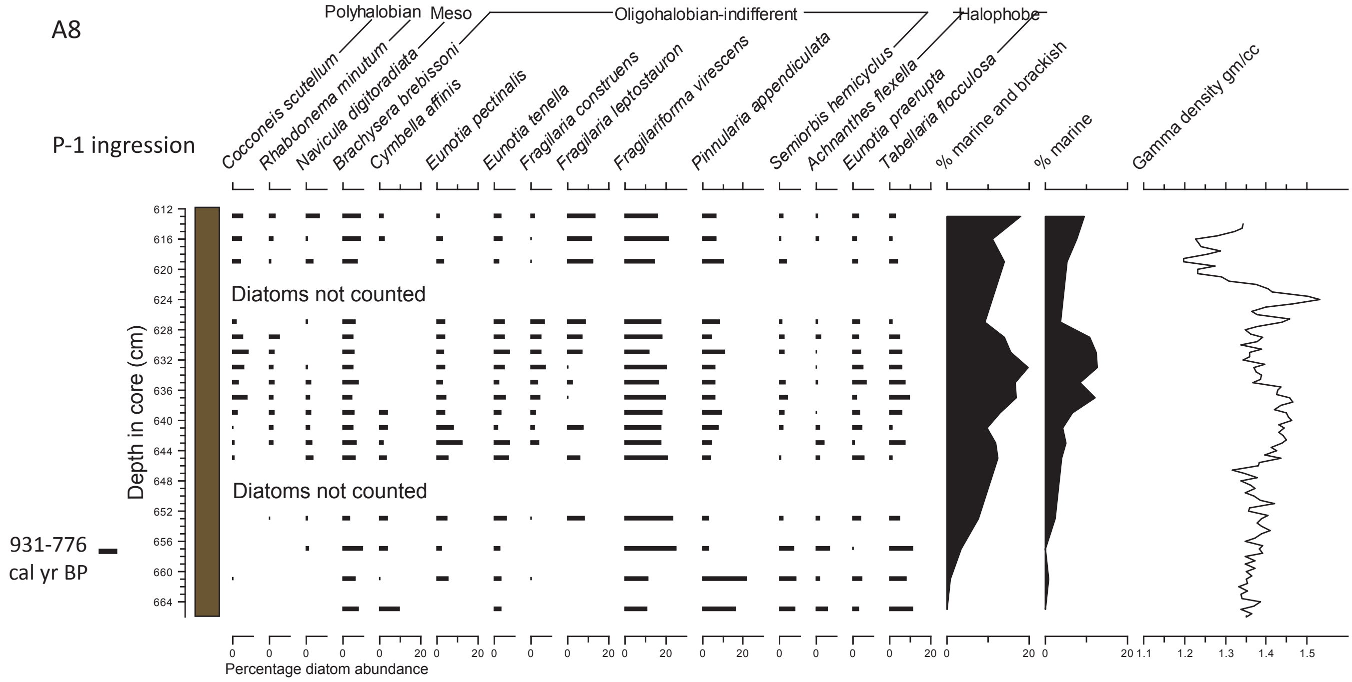

P-1 ingression
Polyhalobian
Meso
Oligohalobian-indifferent
Halophobe
Cocconeis scutellum
Rhabdonema minutum
Navicula digitoradiata
Brachysera brebissoni
Cymbella affinis
Eunotia pectinalis
Eunotia tenella
Fragilaria construens
Fragilaria leptostauron
Fragilariforma virescens
Pinnularia appendiculata
Semiorbis hemicyclus
Achnanthes flexella
Eunotia praerupta
Tabellaria flocculosa
% marine and brackish
% marine
Gamma density gm/cc
Diatoms not counted
Diatoms not counted
Depth in core (cm)
931-776 cal yr BP
Percentage diatom abundance

A9

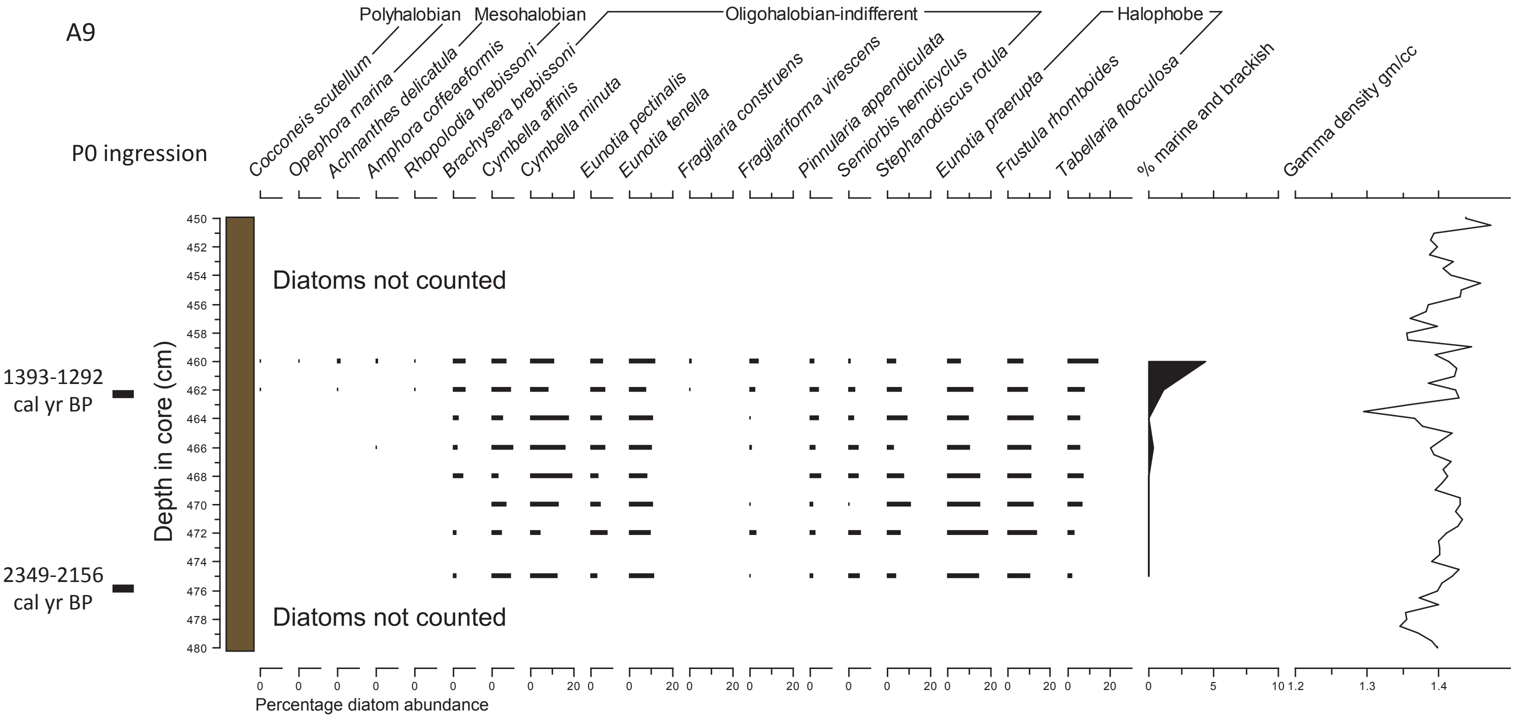

P0 ingression
Polyhalobian
Mesohalobian
Oligohalobian-indifferent
Halophobe
Cocconeis scutellum
Opephora marina
Achnanthes delicatula
Amphora coffeaeformis
Rhopolodia brebissoni
Brachysera brebissoni
Cymbella affinis
Cymbella minuta
Eunotia pectinalis
Eunotia tenella
Fragilaria construens
Fragilariforma virescens
Pinnularia appendiculata
Semiorbis hemicyclus
Stephanodiscus rotula
Eunotia praerupta
Frustula rhomboides
Tabellaria flocculosa
% marine and brackish
Gamma density gm/cc
Diatoms not counted
Diatoms not counted
Depth in core (cm)
1393-1292 cal yr BP
2349-2156 cal yr BP
Percentage diatom abundance